

Chemical analysis of CH stars - I: atmospheric parameters and elemental abundances

Drisya Karinkuzhi^{1,2}, Aruna Goswami¹

¹ *Indian Institute of Astrophysics, Koramangala, Bangalore 560034, India; drisya@iiap.res.in, aruna@iiap.res.in*

² *Department of physics, Bangalore university, Jnana Bharathi Campus, Karnataka 560056, India*

Accepted —; Received —; in original form —

ABSTRACT

Results from high-resolution spectral analyses of a selected sample of CH stars are presented. Detailed chemical composition studies of these objects, which could reveal abundance patterns that in turn provide information regarding nucleosynthesis and evolutionary status, are scarce in the literature. We conducted detailed chemical composition studies for these objects based on high resolution ($R \sim 42\,000$) spectra. The spectra were taken from the ELODIE archive and cover the wavelength range from 3900 Å, to 6800 Å, in the wavelength range. We estimated the stellar atmospheric parameters, the effective temperature T_{eff} , the surface gravity $\log g$, and metallicity $[Fe/H]$ from Local thermodynamic equilibrium analyses using model atmospheres. Estimated temperatures of these objects cover a wide range from 4550 K to 6030 K, the surface gravity from 1.8 to 3.8 and metallicity from -0.18 to -1.4 . We report updates on elemental abundances for several heavy elements and present estimates of abundance ratios of Sr, Y, Zr, Ba, La, Ce, Pr, Nd, Sm, Eu and Dy with respect to Fe. For the object HD 188650 we present the first abundance analyses results based on a high resolution spectrum. Enhancements of heavy elements relative to Fe, that are characteristic of CH stars are evident from our analyses for most of the objects. A parametric model based study is performed to understand the relative contributions from the s- and r-processes to the abundances of the heavy elements.

Key words: stars: Abundances - stars: Carbon - stars: Late-type - stars: Population II.

1 INTRODUCTION

CH stars characterized by iron deficiency, enhanced carbon and s-process elements are known to be post-mass-transfer binaries (McClure & Woodsworth 1990) in which the companion (primary) has evolved to white dwarf passing through an AGB stage of evolution. The chemical composition of CH stars (secondaries) bear the signature of the nucleosynthesis processes occurring in the companion AGB stars due to mass transfer. Two suggested mass transfer mechanisms include Roche-lobe overflow and wind accretion. Recent hydrodynamical simulations have shown in the case of the slow and dense winds, typical of AGB stars, that efficient wind mass transfer is possible through a mechanism called wind Roche-lobe overflow (WRLOF) (Abate et al. 2013 and references therein). CH stars (secondaries) thus form ideal targets for studying the operation of s-process occurring in AGB stars. Chemical abundances of key elements such as Ba, Eu etc. and their abundance ratios could provide insight in this regard. However, literature survey shows

that detailed chemical composition studies of many of the objects belonging to the CH star catalogue of Bartkevicius (1996) are currently not available. A few studies that exist are either limited by resolution or wavelength range. We have therefore undertaken to carry out chemical composition studies for a selected sample of CH stars from this catalogue using high resolution spectra. In our previous studies along this line we have considered the sample of faint high latitude carbon stars of Hamburg/ESO survey (Christlieb et al. 2001) and based on medium resolution spectroscopy found about 33 per cent of the objects to be potential CH star candidates (Goswami 2005, Goswami et al. 2007, 2010). Chemical composition of two objects from this sample based on high resolution Subaru spectra are discussed in Goswami et al. 2006.

CH stars (with $-0.2 < [Fe/H] < -2$) and the class of carbon-enhanced metal-poor (CEMP)-s stars of the CEMP stars classification of Beers & Christlieb (2005) are believed to have a similar origin as far as their chemical composition

is concerned and that, the CEMP-s stars are thought to be more metal-poor counterparts of CH stars. High resolution spectroscopic analyses of carbon-enhanced metal-poor (CEMP) stars have established that the largest group of CEMP stars are s-process rich (CEMP-s) stars and accounts for about 80 per cent of all CEMP stars (Aoki et al. 2007). Chemical composition studies of carbon-enhanced metal-poor stars (Barbuy et al. 2005; Norris et al. 1997a, b, 2002; Aoki et al. 2001, 2002a,b; Goswami et al. 2006, Goswami & Aoki 2010) also have suggested that a variety of production mechanisms are needed to explain the observed range of elemental abundance patterns in them; however, the binary scenario of CH star formation is currently considered as also the most likely formation mechanism for CEMP-s stars. This idea has gained further support with the demonstration by Lucatello et al. (2005b), that the fraction of CEMP-s stars with detected radial-velocity variations is consistent with the hypothesis of all being members of binary systems.

Among CEMP stars the group of CEMP-r/s stars show enhancement of both r- and s-process elements ($0 < [\text{Ba}/\text{Eu}] < 0.5$ (Beers & Christlieb 2005)). Two objects in our sample are found to show $[\text{Ba}/\text{Eu}]$ ratios in this range. Elements heavier than iron are mainly produced by two neutron-capture processes, the slow neutron-capture process (s-process) and the rapid neutron-capture process (r-process). They require entirely different astrophysical environments, different time-scales and different neutron fluxes. While slow neutron-capture elements are believed to be produced in the inter pulse phases of low mass AGB stars, the rapid neutron-capture process requires very high temperatures and neutron flux and are expected to be produced during supernova explosions. To understand the contribution of these two processes to the chemical abundance of the neutron-capture elements we have conducted a parametric model based study. Our study indicates three objects in our sample to have abundances of heavy elements with major contributions coming from the s-process.

Section 2 describes the source of our high resolution spectra. Radial velocity estimates are presented in section 3. Temperature estimates from photometry are discussed in section 4. Determination of stellar atmospheric parameters are presented in section 5. Results of abundance analysis are discussed in section 6. In section 7 we present brief discussions on each individual star. A discussion on the parametric model based analysis is presented in section 8. Conclusions are drawn in section 9.

2 HIGH RESOLUTION SPECTRA OF THE PROGRAM STARS

Program stars are selected from the CH star catalogue of Bartkevičius (1996); the basic data of these objects are listed in Table 1. The spectra are taken from the Elodie archive (Moultaka et al. (2004)). We have considered only those CH stars for which high resolution spectra are available in the archive with S/N ratio > 20 . ELODIE is an echelle spectrograph used at the 1.93 m telescope of Observatoire de Haute Provence (OHP). Optimal extraction and wavelength calibration of data are automatically performed by the online reduction software TACOS. The spectra recorded in a single exposure as 67 orders on a 1K CCD have a resolution of R

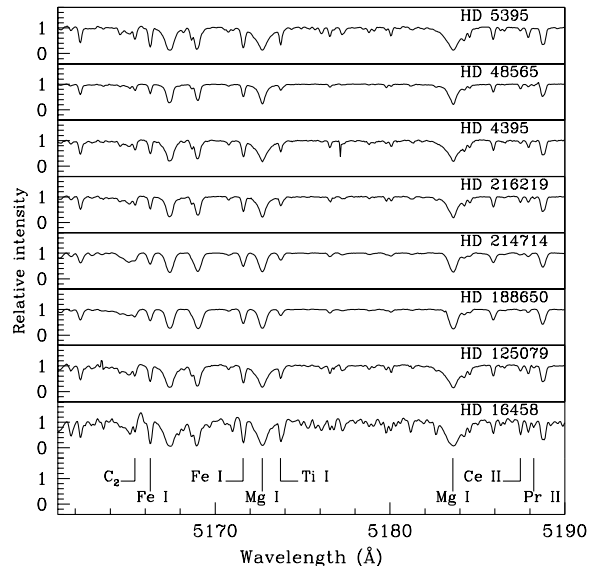


Figure 1. Sample spectra of a few program stars in the wavelength region 5160 to 5190 Å.

~ 42000 . The wavelength range spans from 3900 Å, to 6800 Å. A few sample spectra are shown in Figures 1 and 2.

3 RADIAL VELOCITY

Radial velocities of our program stars are calculated using a selected set of clean unblended lines in the spectra. Estimated mean radial velocities along with the standard deviation from the mean values are presented in Table 2. The literature values are also presented in for a comparison. Radial velocity variations are reported in McClure (1984, 1997) and McClure & Woodworth (1990) for four stars, HD 16458, 201626, 216219 and 4395. Our radial velocity estimate for HD 48565 shows a difference of $\sim 6 \text{ km s}^{-1}$ from the literature value. Variation in radial velocity for this object was also reported by North et al. (1994), and Nordstroem et al. (2004). For the remaining stars we note a small difference from the literature values. Except for HD 201626 (-141.6 km s^{-1}) and HD 81192 (-136.5 km s^{-1}), the program stars are low-velocity objects.

4 TEMPERATURES FROM PHOTOMETRIC DATA

We used colour-temperature calibrations of Alonso, Arribas & Martinez-Roger (1996) that relate T_{eff} with various optical and near-IR colours. Estimated uncertainty in the temperature calibrations is $\sim 100 \text{ K}$. The Alonso et al. calibrations use Johnson photometric systems for UBVR and use TCS (Telescopio Carlos Sanchez) system for IR colours, J-H and J-K. The necessary transformations between these photometric systems are performed using transformation relations from Ramirez & Melendez (2004) and Alonso et al. (1996, 1999). The $B - V$ colour of a star with strong molecular carbon absorption features depends not only on T_{eff} , but

Table 1: Basic data for the program stars

Star Name.	RA(2000)	DEC(2000)	B	V	J	H	K
HD4395	00 46 13.7498	-11 27 08.567	8.39	7.70	6.394	6.099	5.972
HD5395	00 56 39.9051	+59 10 51.800	5.576	4.632	3.123	2.680	2.468
HD16458	02 47 47.7083	+81 26 54.512	7.122	5.790	3.840	3.343	3.032
HD48565	06 44 54.9224	+20 51 38.353	7.732	7.204	6.122	5.884	5.806
HD81192	09 24 45.3354	+19 47 11.866	7.455	6.539	4.846	4.282	4.119
HD125079	14 17 20.7163	-04 15 57.819	9.57	8.67	7.136	6.759	6.610
HD188650	19 54 48.2509	+36 59 44.434	6.528	5.793	4.626	4.111	4.114
HD201626	21 09 59.2714	+26 36 54.928	9.20	8.13	6.315	5.838	5.736
HD214714	22 39 34.3326	+37 35 34.140	6.865	6.038	-	-	-
HD216219	22 50 52.1513	+18 00 07.585	8.06	7.44	6.265	6.034	5.935

Table 2: Radial velocities

Star Name	V_r km s ⁻¹ our estimates	V_r km s ⁻¹ from literature	References
HD 4395	-0.8 ± 0.8	-1.3	4
HD 5395	-47.8 ± 0.9	-47.0	5
HD 16458	18.2 ± 0.5	18	2
HD 48565	-25.7 ± 0.4	-19.4	4
HD 81192	136.5 ± 0.3	135.3	2
HD 125079	-4.5 ± 0.2	-4.3	1
HD 188650	-24.6 ± 0.4	-23.8	2
HD 201626	-141.6 ± 1.2	-145.7	4
HD 214714	-7.0 ± 0.5	-6.8	2
HD 216219	-6.8 ± 0.7	-7.5	3

1. Smith et al. (1993) 2. Wilson (1953) 3. De Medeiros & Mayor (1999) 4. Nordström et al. (2004) 5. Masseroni et al. (2008)

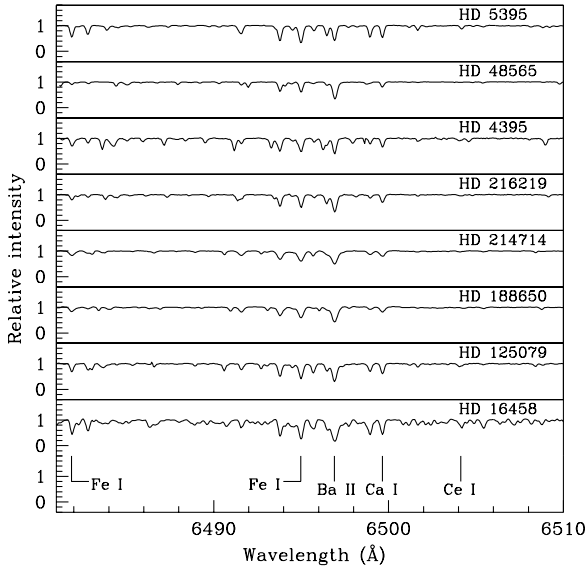


Figure 2. Spectra showing the wavelength region 6480 to 6510 Å, for the same stars as in Figure 1.

also on the metallicity of the star and on the strength of its molecular carbon absorption features, due to the effect of CH molecular absorption in the B band. The derived T_{eff} from V-K is ~ 450 K, and from J-H is ~ 250 K lower than the adopted spectroscopic T_{eff} derived by imposing Fe I excitation equilibrium. The temperature calibrations from the $T_{\text{eff}} - (J-H)$ and $T_{\text{eff}} - (V-K)$ relations involve a metallicity

([Fe/H]) term. Estimates of T_{eff} at two assumed metallicity values (shown in parenthesis) are listed in Table 3.

5 STELLAR ATMOSPHERIC PARAMETERS

A set of Fe I and Fe II lines with excitation potential in the range 0.0 - 5.0 eV and equivalent width 20 Å to 180 Å were selected to find the stellar atmospheric parameters. These lines are listed in Table 4. Throughout our analysis we have assumed local thermodynamic equilibrium (LTE). A recent version of MOOG of Sneden (1973) is used for the calculations. Model atmospheres were selected from the Kurucz grid of model atmospheres with no convective overshooting. These are available at <http://cfaku5.cfa.harvard.edu/> labelled with a suffix odnew. Solar abundances are taken from Asplund et al. (2005).

The microturbulent velocity was estimated at a given effective temperature by demanding that there be no dependence of the derived Fe I abundance on the equivalent width of the corresponding lines.

The effective temperature is determined by making the slope of the abundance versus excitation potential of Fe I lines to be nearly zero. The initial value of temperature is taken from the photometric estimates and arrived at a final value by an iterative method with the slope nearly equal to zero. Figures 3 and 4 show abundance of Fe I and Fe II as a function of excitation potential and equivalent widths respectively.

The surface gravity was fixed at a value that gives same abundances for Fe I and Fe II lines. Clean Fe II lines are more

Table 3: Temperatures from photometry

Star Name	T_{eff} K (J-K)	$T_{eff}(-0.5)$ K (J-H)	$T_{eff}(-0.5)$ K (V-K)	$T_{eff}(-1.0)$ K (J-H)	$T_{eff}(-1.0)$ K (V-K)	$T_{eff}(-0.5)$ K (B-V)	$T_{eff}(-1.0)$ K (B-V)	Spectroscopic estimates (K)
HD 4395	5496.71	5776.28	5398.05	5791.79	5392.69	5365.08	5243.37	5550
HD 5395	4556.52	4950.59	4842.04	4967.30	4829.76	4666.20	4563.87	4860
HD 16458	4082.41	4713.82	4216.43	4730.59	4198.88	3886.55	3804.68	4550
HD 48565	6047.46	6150.12	5891.51	6164.60	5894.11	5928.43	5790.39	6030
HD 81192	4321.94	4382.20	4555.65	4398.88	4540.63	4734.38	4630.20	4870
HD 125079	5037.98	5285.39	4964.79	5301.79	4953.86	4774.22	4668.96	5520
HD 188650	5095.69	4553.41	5469.31	4570.17	5464.99	5226.76	5108.96	5700
HD 201626	4829.70	4754.07	4581.24	4770.85	4566.44	4381.70	4286.98	5120
HD 214714	—	—	—	—	—	4964.61	4854.13	5550
HD 216219	5969.13	6209.69	5723.41	6223.98	5723.10	5595.08	5466.79	5960

The numbers in the parenthesis indicate the metallicity values at which the temperatures are calculated.

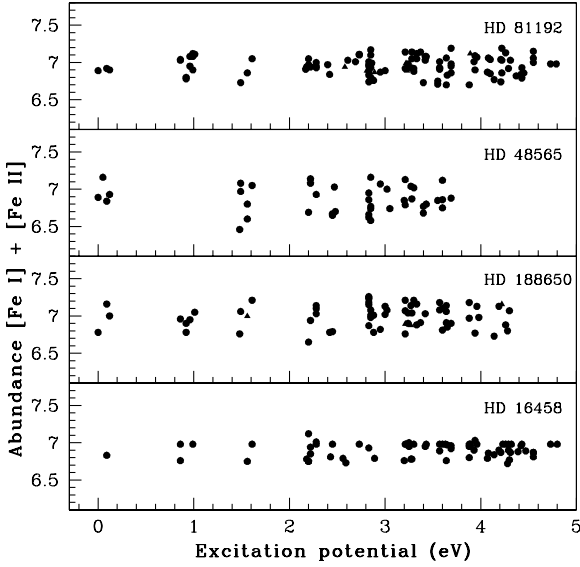


Figure 3. The iron abundances of stars are shown for individual Fe I and Fe II lines as a function of excitation potential. The solid circles indicate Fe I lines and solid triangles indicate Fe II lines.

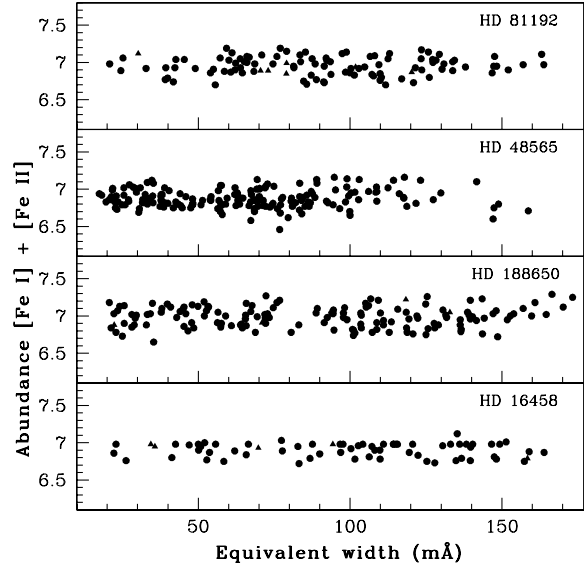


Figure 4. The iron abundances of stars are shown for individual Fe I and Fe II lines as a function of equivalent width. The solid circles indicate Fe I lines and solid triangles indicate Fe II lines.

difficult to find than Fe I lines, so we were limited to 4-10 Fe II lines for the abundance analysis in most cases.

6 ABUNDANCE ANALYSIS

Abundances for most of the elements are determined from the measured equivalent widths of lines due to neutral and ionized elements using a recent version of MOOG of Sneden (1973) and the adopted model atmospheres. A master line list including all the elements is generated comparing the spectra of the program stars with the spectrum of Arcturus. The presented line lists contain only those lines which are used for abundance calculation. In most of the spectra we could get very few usable clean lines. The log gf values for the atomic lines were adopted from various sources which include Aoki et al. (2005, 2007), Goswami et al. (2006), Jonsell et al. (2006), Luck & Bond (1991) and Sneden et al. (1996), whenever available, and also from Kurucz atomic line database (Kurucz 1995a,b). The log gf values for a few La lines are taken from Lawler,

Bonvallet & Sneden (2001). We determined abundances for Na, Mg, Ca, Sc, Ti, V, Cr, Mn, Co, Ni, Zn and for heavy elements Sr, Y, Zr, Ba, La, Ce, Pr, Nd, Sm, Eu and Dy. For the elements Sc, V, Mn, Ba, La and Eu, spectrum synthesis was used to find the abundances considering hyperfine structure. The line lists for each region that is synthesized are taken from Kurucz atomic line list (<http://www.cfa.harvard.edu/amdata/ampdata/kurucz23/sekur.html>). As an example, spectrum synthesis calculations for Sc, Ba and La are shown in Figures 5, 6 and 7.

Derived abundance ratios with respect to iron are listed in Table 6. In Table 7, we have presented [ls/Fe], [hs/Fe] and [hs/ls] values, where ls represents light s-process elements Sr, Y and Zr and hs represents heavy s-process elements Ba, La, Ce, Nd and Sm. Lines used for the abundance calculation of these elements are listed in Tables 8 and 9.

Table 4: Fe lines used for deriving atmospheric parameters

Wavelength	Element	E_{low}	log gf	HD 4395	HD 5395	HD 16458	HD 48565	HD 81192	HD 125079	HD 188650	HD 201626	HD 214714	HD 216219
4114.440	Fe I	2.830	-1.300	-	-	-	57.9	91.4	-	-	-	115.5	-
4132.900		2.850	-1.010	-	-	-	72.2	-	-	-	-	-	96.4
4143.870		1.560	-0.510	-	-	-	147.1	-	-	-	-	-	-
4147.670		1.490	-2.100	-	-	-	89.1	120.9	-	-	-	-	-
4153.900		3.400	-0.320	-	-	-	76.9	-	-	-	-	-	-
4154.500	Fe I	2.830	-0.690	-	-	-	79.6	-	-	-	-	-	-
4184.890		2.830	-0.870	113.7	-	-	-	-	-	143.5	-	134.7	104.5
4187.040		2.450	-0.550	-	-	-	100.0	-	-	-	-	-	137.7
4216.180		0.000	-3.360	-	-	-	88.4	-	-	-	-	-	-
4202.030		1.490	-0.710	-	-	-	-	-	-	-	130.2	-	-
4337.050	Fe I	1.560	-1.700	124.3	-	-	-	-	-	-	-	-	125.5
4438.345		3.882	-1.630	-	-	-	-	-	-	29.2	-	42.7	-
4427.310		0.050	-2.920	-	-	-	117.9	-	-	-	-	-	-
4422.567		2.845	-1.110	-	-	-	-	123.5	-	-	-	-	-
4445.470		0.087	-5.380	-	-	122.4	-	-	-	39.8	-	-	-
4446.833	Fe I	3.687	-1.330	-	-	-	34.1	77.0	-	-	-	-	51.5
4447.720		2.220	-1.340	-	-	-	98.9	138.0	-	141.6	38.5	-	-
4454.380		2.832	-1.250	-	-	-	70.0	101.4	-	-	-	-	88.7
4461.653		0.087	-3.210	137.6	-	-	92.3	-	-	-	-	-	-
4466.551		2.832	-0.590	-	-	-	100.3	147.3	-	160.9	91.8	160.1	125.5
4484.220	Fe I	3.602	-0.720	81.4	-	-	63.2	83.7	95.3	94.7	49.7	-	77.7
4489.739		0.121	-3.966	-	-	-	67.5	123.6	-	122.0	-	-	-
4531.150		1.490	-2.150	-	-	-	87.2	-	-	-	-	-	-
4547.846		3.546	-0.780	-	-	-	54.2	85.7	96.5	-	-	-	-
4566.514		3.301	-2.250	-	-	55.7	-	-	-	-	-	-	-
4574.215	Fe I	3.211	-2.500	28.1	55.9	-	-	-	-	23.4	-	35.1	-
4587.128		3.573	-1.780	51.3	-	-	-	55.0	-	44.9	-	60.7	44.5
4595.358		3.301	-1.720	57.9	-	-	38.9	68.3	-	76.7	-	56.1	65.9
4596.060		3.602	-1.640	-	-	-	34.7	-	-	-	-	57.2	-
4619.287		3.602	-1.120	-	-	-	41.8	-	-	89.2	-	-	74.5
4625.044	Fe I	3.241	-1.340	-	-	-	-	88.5	-	94.0	-	-	-
4630.121		2.278	-2.600	-	-	-	38.1	81.5	-	72.8	-	92.2	-
4632.911		1.608	-2.913	-	-	-	57.6	-	-	109.3	-	-	-
4635.846		2.845	-2.420	-	-	-	-	63.9	-	42.7	-	65.6	33.7
4643.463		3.654	-1.290	-	82.8	-	-	-	-	57.4	-	73.1	52.3
4690.140	Fe I	3.686	-1.640	-	67.5	-	23.0	53.9	-	-	-	-	44.4
4710.280		3.018	-1.610	-	-	-	57.3	-	-	94.5	-	-	-
4733.591		1.484	-2.710	-	-	-	57.3	-	-	-	-	114.0	92.5
4736.772		3.211	-0.740	-	-	-	89.0	125.8	-	139.6	-	-	-
4741.529		2.832	-2.000	71.2	-	-	-	83.7	-	65.8	-	67.2	-
4745.800	Fe I	3.654	-0.790	-	-	-	48.2	87.2	-	-	-	-	-
4768.319		3.686	-1.109	-	-	102.7	45.9	-	-	72.2	-	88.3	-
4787.833		3.000	-2.770	-	-	-	-	-	-	24.2	-	30.5	-
4788.760		3.237	-1.760	63.0	87.3	-	31.6	-	-	57.6	-	-	57.9
4789.650		3.546	-0.910	87.7	-	-	-	84.7	-	-	-	-	-
4842.788	Fe I	4.104	-1.560	41.1	-	-	-	45.4	-	-	-	-	-
4871.318		2.865	-0.360	-	-	-	108.8	-	-	-	-	-	145.2
4875.870		3.332	-2.020	53.2	71.4	-	25.5	63.8	-	32.9	-	44.3	45.9
4882.140		3.417	-1.640	-	80.2	107.2	31.7	75.9	-	-	-	63.8	51.3
4896.440		3.884	-2.050	-	-	-	-	-	-	20.7	-	34.9	-
4903.310	Fe I	2.883	-0.930	-	-	-	84.5	144.9	-	139.2	-	139.5	110.2
4907.737		3.430	-1.840	56.7	81.5	-	22.3	-	-	-	-	-	46.6
4908.029		4.217	-1.285	33.4	-	-	-	-	-	-	-	-	-
4917.229		4.191	-1.180	58.4	55.0	-	28.5	-	-	49.9	72.8	65.6	142.4
4924.770		2.279	-2.256	92.1	-	151.4	54.2	-	-	106.1	-	108.6	-
4930.315	Fe I	3.959	-1.350	-	-	-	29.4	69.9	-	53.2	-	69.4	-
4939.690		0.859	-3.340	-	147.5	-	63.1	127.2	122.1	119.4	-	131.7	88.5
4967.890		4.191	-0.622	70.8	89.1	108.1	43.4	-	80.4	-	-	73.9	63.5
4969.916		4.216	-0.710	69.5	90.2	-	38.9	-	-	-	-	-	61.9
4985.250		3.928	-0.560	91.9	110.2	109.8	57.4	93.5	-	-	-	-	-
5001.860	Fe I	3.881	0.090	-	-	-	77.8	111.7	126.6	-	65.2	-	-
5005.711		3.883	-0.180	100.8	-	-	74.1	-	132.3	-	-	-	98.2
5006.119		2.833	-0.610	146.8	-	-	98.5	157.0	-	173.3	-	-	128.4
5007.728		4.294	-1.502	-	-	-	-	-	50.0	-	-	-	-
5022.235		3.984	-0.530	91.1	-	-	59.5	-	-	97.8	-	-	-
5028.126	Fe I	3.573	-1.474	-	-	-	-	-	-	75.9	-	-	60.1
5031.915		4.372	-1.670	-	37.2	-	-	-	-	-	-	24.7	-
5044.210		2.851	-2.150	72.1	-	-	-	83.5	-	65.6	-	79.9	-
5049.820		2.279	-1.344	136.0	-	-	86.5	-	-	157.0	-	161.8	115.2
5051.635		0.915	-2.795	-	-	-	87.6	-	-	-	95.9	-	-
5054.640	Fe I	3.639	-2.140	37.1	55.7	-	-	-	-	25.6	-	35.1	24.7
5079.224		2.198	-2.067	-	-	-	70.1	-	-	-	-	-	-
5083.338		0.958	-2.958	104.3	157.2	-	74.6	147.6	-	136.3	-	-	98.6
5088.166		4.155	-1.780	-	-	-	-	-	-	-	-	26.62	-
5109.650		4.301	-0.980	59.8	-	-	35.2	-	-	52.7	-	-	-
5127.360	Fe I	0.920	-3.310	94.6	148.6	-	64.7	117.0	120.4	107.3	-	-	-
5141.739		2.424	-2.150	87.1	114.1	-	48.1	93.71	-	80.6	-	102.8	76.4
5151.910		1.011	-3.320	-	-	-	63.0	-	-	118.5	-	-	-
5159.050		4.283	-0.820	52.3	79.2	83.2	32.8	-	-	46.6	-	67.1	57.6
5166.282		0.000	-4.195	111.9	-	-	72.0	133.8	-	112.9	79.1	129.0	-
5171.600	Fe I	1.485	-1.790	156.3	-	-	108.5	-	-	178.4	103.1	164.4	135.1
5192.343		3.000	-0.420	-	-	-	108.8	-	-	164.6	-	163.2	-
5187.914		4.143	-1.260	53.8	-	-	19.6	-	-	25.02	-	38.5	-
5194.941		1.557	-2.090	119.9	170.0	-	83.3	146.8	-	151.8	-	142.7	114.4
5195.468		4.220	-0.020	89.1	111.2	-	62.0	-	-	-	-	-	89.1
5198.711	Fe I	2.223	-2.135	98.3	-	-	57.5	121.5	-	103.5	-	113.0	83.3
5215.179		3.266	-0.933	-	131.9	148.2	69.8	-	-	108.8	-	119.6	98.3
5228.403		4.221	-1.290	-	-	-	-	59.3	-	40.9	-	53.13	-
5226.862		3.038	-0.667	-	-	-	103.0	-	-	-	-	-	-
5232.939		2.940	-0.060	-	-	-	127.4	-	-	-	-	-	167.4
5250.645	Fe I	2.198	-2.050	-	-	-	-	-	-	113.6	-	130.3	74.9
5247.050		0.087	-4.980	-	-	-	22.9	100.3	-	-	-	-	-
5242.490		3.630	-0.970	74.2	-	111.0	50.9	-	-	-	-	90.8	-
5253.461		3.283	-1.670	73.8	-	109.9	35.2	85.4	-	60.9	-	73.4	61.7
5263.305		3.265	-0.970	105.5	-	-	68.5	-	-	101.1	67.5	103.2	93.9
5266.555	Fe I	2.998	-0.490	106.1	-	-	-	-	-	-	152.2	127.2	-
5281.800		3.040	-0.833	128.0	-	-	81.9	147.2	-	125.0	76.3	131.9	112.1
5283.630		3.240	-0.524	-	-	-	95.3	-	-	147.1	-	148.1	-
5324.178		3.211	-0.240	-	-	-	112.5	172.4	-	170.2	98.85	169.2	-
5307.370		1.610	-2.912	85.3	130.0	149.3	47.5	112.5	107.6	99.0	57.19	104.6	73.1

Table 4 : continued

Wavelength	Element	E_{low}	log gf	HD 4395	HD 5395	HD 16458	HD 48565	HD 81192	HD 125079	HD 188650	HD 201626	HD 214714	HD 216219
5321.110		4.434	-1.090	39.3	53.7	-	-	39.9	-	22.9	-	35.1	30.3
5322.040		2.279	-2.800	55.8	95.7	114.3	-	81.4	75.8	48.5	-	63.0	-
5328.040		0.915	-1.470	-	-	-	147.4	-	-	-	160.5	-	-
5339.928		3.266	-0.680	124.6	148.2	-	83.38	121.5	-	129.1	78.3	134.2	108.2
5364.858		4.446	0.220	107.0	120.8	-	71.3	100.0	119.1	111.0	-	109.2	99.9
5367.479		4.415	0.350	-	123.6	130.5	70.1	107.2	-	118.6	63.4	115.8	104.4
5369.958		4.371	0.350	124.2	136.2	-	84.0	107.7	-	131.5	66.5	134.9	109.6
5373.698		4.473	-0.860	-	72.0	77.6	23.6	-	-	-	-	48.9	47.4
5379.574		3.694	-1.480	-	81.6	100.3	23.2	68.6	67.0	45.3	-	54.5	48.8
5383.369		4.312	0.500	132.6	148.6	163.9	92.7	134.4	143.5	136.3	-	139.4	125.2
5429.710		0.960	-1.881	-	-	-	141.7	-	-	-	140.4	-	-
5434.520		1.011	-2.130	159.5	-	-	102.8	-	-	-	128.4	-	132.5
5464.280		4.143	-1.400	38.6	53.9	-	18.2	-	55.0	-	-	-	36.9
5497.520		1.011	-2.830	-	-	-	-	163.1	-	166.5	-	-	-
5501.464		0.958	-2.950	116.8	-	-	77.1	148.3	151.0	144.2	-	156.8	106.7
5525.539		4.231	-1.330	45.3	66.6	50.0	-	46.3	46.3	33.2	-	37.4	37.3
5543.937		4.217	-1.140	56.3	75.0	-	25.5	60.1	66.2	45.9	-	-	44.9
5554.882		4.548	-0.440	-	-	97.0	-	79.1	-	69.4	-	-	-
5560.207		4.434	-1.190	41.5	-	42.5	17.4	42.3	49.0	51.9	-	40.4	35.93
5567.392		2.608	-2.800	-	-	-	21.7	81.2	-	127.9	-	68.2	49.9
5569.618		3.417	-0.540	124.3	-	-	85.7	128.3	-	110.0	-	124.5	112.0
5576.090		3.430	-1.000	102.3	-	133.1	67.3	106.6	111.5	159.8	90.70	153.2	138.2
5586.756		3.364	-0.210	-	-	-	114.3	-	174.9	-	-	-	152.1
5615.660		3.330	0.050	-	-	-	117.7	-	-	-	-	-	-
5617.186		3.252	-2.880	-	41.3	52.1	-	-	-	-	-	-	-
5618.630		4.209	-1.270	43.2	61.7	-	-	41.8	-	-	-	36.9	32.28
5636.694		3.640	-2.610	-	34.0	26.3	-	25.2	21.5	-	-	-	-
5701.549		2.559	-2.210	-	-	136.7	42.6	-	-	-	-	-	-
5731.765		4.256	-1.300	52.2	-	-	21.8	-	-	38.0	-	46.7	-
5741.848		4.256	-1.730	22.5	45.3	-	-	-	-	-	-	-	-
5753.121		4.260	-0.760	75.2	90.2	87.6	37.8	-	79.5	65.5	-	73.7	65.23
5809.220		3.884	-1.610	45.8	-	82.8	-	70.1	60.2	-	18.9	36.9	33.2
5855.080		4.607	-1.480	25.3	-	-	-	-	24.7	-	-	-	-
5856.100		4.294	-1.560	28.7	-	66.5	-	32.7	40.1	-	-	-	20.1
5862.370		4.550	-0.250	79.4	93.3	106.3	44.7	-	86.2	68.7	-	75.3	70.5
5883.813		3.959	-1.360	57.8	81.4	104.2	30.9	66.8	-	-	-	116.2	49.1
5914.194		4.607	-0.050	-	-	-	-	-	-	105.1	-	-	-
5976.779		3.943	-1.310	-	106.6	-	22.7	62.1	-	-	21.2	-	51.1
6003.017		3.881	-1.120	-	82.0	97.7	37.8	-	88.6	71.9	24.0	72.9	67.8
6024.049		4.548	-0.102	61.7	-	119.5	56.8	92.1	107.3	97.9	39.7	98.0	81.1
6082.710		2.223	-3.550	-	-	90.0	35.6	76.0	50.8	-	-	-	31.0
6136.615		2.453	-1.400	137.6	-	-	86.2	-	-	-	-	-	-
6136.993		2.198	-2.950	75.5	-	125.3	26.9	-	150.6	-	-	-	-
6137.694		2.588	-1.400	-	-	-	80.6	-	-	-	-	-	-
6151.620		2.176	-3.370	32.4	-	101.6	52.2	-	64.3	34.2	83.2	145.9	114.6
6165.360		4.143	-1.460	44.2	60.8	65.7	-	39.1	51.6	25.5	-	32.1	49.3
6180.205		2.727	-2.780	50.5	-	115.6	-	70.9	-	37.8	-	-	28.6
6173.343		2.223	-2.880	67.7	107.5	139.7	25.9	-	85.6	67.3	-	-	40.1
6219.280		2.197	-2.430	90.2	132.1	157.4	51.4	109.5	109.0	103.5	66.9	105.6	54.2
6232.639		3.653	-1.270	78.0	103.1	-	37.4	-	-	64.5	-	80.2	80.2
6230.736		2.559	-1.280	140.6	-	-	86.9	-	-	153.9	-	156.6	68.5
6246.327		3.602	-0.960	-	-	-	62.9	-	-	103.7	-	107.1	121.5
6240.650		2.223	-3.170	-	87.2	-	-	64.9	-	-	-	-	107.1
6252.550		2.404	-1.690	104.0	77.4	-	114.9	158.0	134.1	125.7	-	-	34.0
6254.250		2.278	-2.400	-	-	-	-	-	-	-	-	81.8	131.7
6265.130		2.176	-2.540	-	-	44.18	104.8	103.3	92.4	-	105.9	73.3	-
6246.327		3.602	-0.960	-	-	120.6	-	-	-	-	-	-	-
6270.240		2.858	-2.710	49.2	-	-	-	62.3	-	-	-	-	36.9
6280.630		0.859	-4.390	-	118.2	140.4	-	-	89.4	-	-	-	-
6297.800		2.222	-2.740	-	-	-	33.2	-	86.7	73.4	-	82.6	68.8
6301.498		3.653	-0.740	99.6	-	-	63.6	-	118.1	101.1	-	-	91.1
6318.018		2.453	-2.330	-	-	138.3	-	113.4	-	106.8	-	117.2	-
6322.690		2.588	-2.402	79.4	109.3	127.9	37.74	-	84.7	63.9	43.0	71.0	61.3
6335.340		2.197	-2.230	96.6	141.4	-	56.4	123.4	-	108.8	-	114.4	83.96
6336.823		3.686	-1.050	-	-	-	56.6	-	-	98.2	-	99.2	-
6408.016		3.686	-1.040	90.3	-	-	48.0	-	-	-	-	100.3	76.1
6411.650		3.653	-0.820	-	-	-	70.3	91.5	-	-	-	117.2	-
6419.980		4.733	-0.240	79.7	96.3	114.3	38.6	74.6	86.1	72.1	-	76.8	68.8
6421.350		2.278	-2.030	-	-	-	68.3	127.3	132.6	122.3	75.69	128.9	100.0
6481.869		2.278	-2.984	-	105.2	-	33.2	-	75.5	65.8	-	68.1	48.2
6494.980		2.404	-1.273	-	-	-	94.4	163.8	154.1	148.6	-	166.1	127.7
6574.240		0.990	-5.040	31.7	-	115.1	-	66.0	-	-	-	-	-
6575.022		2.588	-2.820	-	-	-	-	-	-	-	-	-	44.39
6593.880		2.432	-2.420	-	-	147.5	40.02	-	-	-	-	-	73.41
6597.557		4.796	-1.070	-	-	22.9	-	45.0	40.6	-	-	-	-
6627.540		4.548	-1.680	22.9	-	-	-	-	-	-	-	-	-
6677.989		2.692	-1.470	-	-	-	-	133.8	-	138.7	-	-	107.4
6713.750		4.795	-1.390	-	27.0	-	-	20.8	-	-	-	-	-
6725.360		4.103	-2.170	-	27.8	-	-	-	23.7	-	-	-	-
6739.520		1.557	-4.790	-	-	58.4	-	-	23.7	-	-	-	-
6750.150		2.424	-2.620	-	113.5	-	33.9	74.2	81.5	-	-	-	61.1
6752.711		4.640	-1.200	-	-	-	-	-	34.0	-	-	27.0	23.4
6793.260		4.076	-2.330	-	21.2	22.3	-	-	-	-	-	-	-
4233.172	Fe II	2.580	-2.000	-	-	-	97.5	101.8	-	-	76.9	-	-
4491.405		2.855	-2.700	69.1	-	-	64.6	-	-	132.9	45.7	109.5	89.4
4515.339		2.840	-2.480	-	-	-	74.3	-	-	-	-	-	101.5
4520.224		2.810	-2.600	-	-	-	71.7	70.5	-	-	-	-	94.9
4620.510		2.830	-3.290	-	66.4	69.8	-	-	-	-	-	-	-
4629.340		2.807	-2.280	-	-	-	75.8	-	-	99.4	-	130.6	-
4923.930		2.891	-1.320	145.6	161.0	158.4	123.6	120.3	-	-	-	-	165.0
5197.577		3.230	-2.100	-	95.0	-	71.2	73.0	-	-	54.9	131.1	98.1
5534.834		3.245	-2.930	-	-	-	50.6	-	-	118.4	-	100.4	72.9
6247.550		3.891	-2.510	38.3	-	34.4	42.5	-	-	-	-	90.7	-
6369.460		2.891	-4.020	-	26.8	-	-	-	-	-	-	-	-
6416.919		3.891	-2.740	-	46.0	35.7	25.7	30.2	44.0	71.0	-	57.9	49.3
6456.383		3.903	-2.075	57.9	67.8	-	51.4	-	-	-	33.4	-	-

6.1 Carbon

Smith (1984) reported a carbon abundance of 8.70 dex and $C^{12}/C^{13} \sim 15$ for HD 16458. For the three sub-giant CH stars in our sample, HD 125079, 216219 and 4395 carbon abundances and isotopic ratios are available in the litera-

ture (Smith et al. (1993) and Luck & Bond (1982)). Luck & Bond (1982) determined a $[C/Fe]$ value of 0.4 and 1.2 for HD 216219 and 4395 respectively. Smith et al. (1993) gave carbon abundances of 8.65 dex, 9.05 dex, and 9.02 dex for HD 4395, 125079 and 216219 respectively. Vanture (1992a,b)

Table 5: Derived atmospheric parameters for the program stars

Star Name.	T_{eff} K	$\log g$	ζ km s ⁻¹	[Fe I/H]	[Fe II/H]
HD 4395	5550	3.66	0.93	-0.16	-0.19
HD 5395	4860	2.51	1.21	-0.24	-0.24
HD 16458	4550	1.8	1.92	-0.65	-0.66
HD 48565	6030	3.8	1.13	-0.59	-0.59
HD 81192	4870	2.75	1.08	-0.50	-0.51
HD 125079	5520	3.3	1.25	-0.18	-0.18
HD 188650	5700	2.15	2.33	-0.46	-0.44
HD 201626	5120	2.25	1.02	-1.39	-1.41
HD 214714	5550	2.41	1.96	-0.35	-0.36
HD 216219	5950	3.5	1.31	-0.17	-0.18

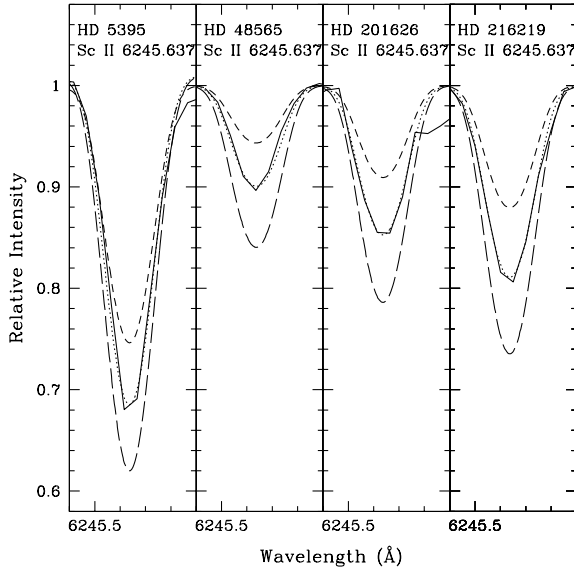


Figure 5. Spectral-synthesis fits of Sc II line at 6245.637 Å. The dotted lines indicate the synthesized spectra and the solid lines indicate the observed line profiles. Two alternative synthetic spectra for $[X/Fe] = +0.3$ (long-dashed line) and $[X/Fe] = -0.3$ (short-dashed line) are shown to demonstrate the sensitivity of the line strength to the abundances.

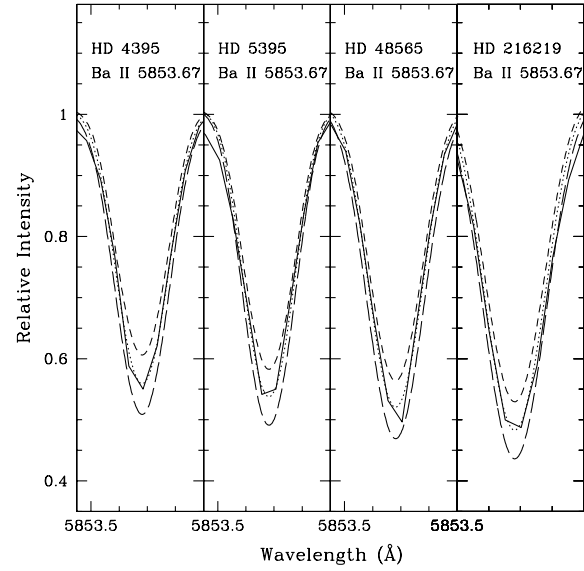


Figure 6. Spectral-synthesis fits of Ba II line at 5853.67 Å. The dotted lines indicate the synthesized spectra and the solid lines indicate the observed line profiles. Two alternative synthetic spectra for $[X/Fe] = +0.3$ (long-dashed line) and $[X/Fe] = -0.3$ (short-dashed line) are shown to demonstrate the sensitivity of the line strength to the abundances.

reported a carbon abundance of 8.4 dex and $C^{12}/C^{13} \sim 25$ for the object HD 201626. Luck (1991) gives a $[C/H] \sim -0.16$ and $C^{12}/C^{13} \sim 25$ for HD 214714. Baird et al. (1975) also noticed an enhancement of carbon in HD 214714 and 188650 with respect to β Aqr. Because of the carbon deficiency in β Aqr they concluded that these two stars show normal carbon abundances. For HD 81192, Cottrell and Sneden (1986) reported a C/N ratio of 11.2 and Shetrone, Sneden & Pilachowski (1993) gave $C^{12}/C^{13} \sim 35$.

6.2 Na and Al

The sodium (Na) abundances were calculated using the lines at 5682.65 Å and 5688.22 Å in the case of six objects. For HD 48565 a single line at 5682.65 Å is used. As these lines could not be used for HD 5395 and HD 81192, the resonant doublet lines at 5890.9 and 5895.9 Å are used. For HD 201626 the line at 5895.9 Å is used which is observed as

a broad line with an equivalent width of 214 mÅ. We have used LTE analysis for the abundance determination. However, the resonance lines are sensitive to non-LTE effects (Baumüller & Gehren 1997; Baumüller, Butler & Gehren 1998; Cayrel et al. 2004). Derived Na abundances from LTE analysis range from -0.23 to 0.76 in the present sample. We note that Na in HD 5395 and HD 81192 is found to be underabundant with respect to Fe while the other stars show mild over abundances.

Al lines in our spectral region are blended and could not be used for abundance determination.

6.3 Mg, Si, Ca, Sc, Ti, V

We could measure several lines due to these elements. Except for HD 201626, that shows an overabundance of Mg with $[Mg/Fe] \sim 0.69$, all other stars show mild enhancement or near-solar value of Mg. None of the Si lines detected in

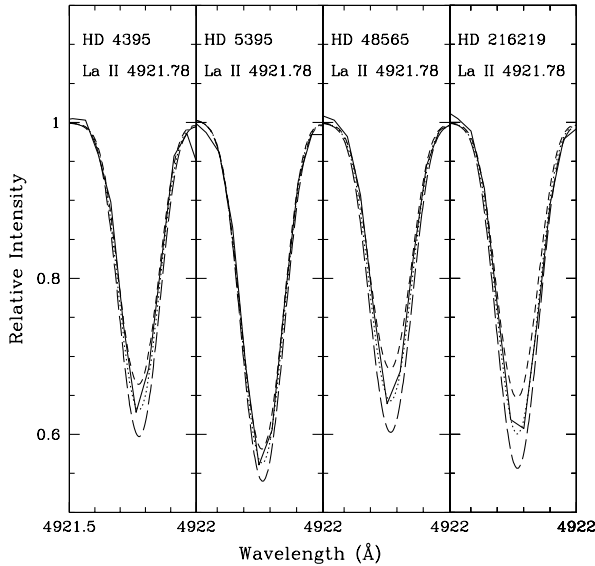


Figure 7. Spectral-synthesis fits of La II line at 4921.78 Å. The dotted lines indicate the synthesized spectra and the solid lines indicate the observed line profiles. Two alternative synthetic spectra for $[X/Fe] = +0.3$ (long-dashed line) and $[X/Fe] = -0.3$ (short-dashed line) are shown to demonstrate the sensitivity of the line strength to the abundances.

our spectra was found to be usable for abundance determination. Ca shows a mild enhancement or near-solar value in these objects except for HD 201626, which shows an overabundance of Ca with $[Ca/Fe] \sim 0.65$.

Sc abundance is determined using spectrum synthesis calculation of Sc II line at 6245.63 Å considering hyperfine structure from Prochaska and McWilliam (2000). While Sc is found to be mildly underabundant in HD 188650 and HD 214714 with $[Sc II/Fe] \sim -0.5$, the other stars show nearly solar values.

Except for HD 201626, the program stars show a mild overabundance or near-solar abundance for Ti measured using more than ten lines. HD 201626 shows an overabundance of Ti with $[Ti/Fe] \sim 0.8$.

We detected more than 16 V I lines but only one or two usable lines of V I for the determination of V abundance; other lines appear either blended or distorted in the spectra. Abundance of V is estimated from spectrum synthesis calculation of V I line at 5727.048 Å taking into account the hyperfine components from Kurucz database for all the program stars except HD 201626. V abundance could not be estimated for HD 201626 due to severe line blending. While HD 16458 shows $[V/Fe] \sim 0.25$ all other program stars show mild under abundance or nearly solar values for V.

6.4 Cr, Co, Mn, Ni, Zn

HD 16458 shows a mild overabundance of Cr relative to Fe. HD 125079, 188650, 216219, and 4395 show near-solar abundances. The rest of the stars in our sample are mildly underabundant in Cr. HD 201629 however shows a larger underabundance with $[Cr/Fe] = -0.59$. Cr abundances mea-

sured using Cr II lines whenever possible also show similar trends.

Mn abundance is calculated using spectrum synthesis calculation of 6013.51 Å line considering hyperfine structures from Prochaska & McWilliam (2000). Except for HD 16458, that shows near solar abundance with $[Mn/Fe] \sim 0.06$, the rest show underabundance of Mn with $[Mn/Fe] \leq -0.22$.

Except for HD 16458 with $[Co/Fe] \sim 0.49$, all other stars in our sample show near-solar values for Co.

Abundances of Ni measured from Ni I lines give near-solar values for all the stars.

HD 16458 and 5395 show mild overabundance with $[Zn/Fe] \sim 0.43$ and 0.29 respectively. The rest of the objects show near solar values.

6.5 Sr, Y, Zr

The Sr abundance was derived from Sr I line at 4607.327 Å for seven stars. HD 16458, 125079, 4395, 48565 and 216219 show overabundances with $[Sr/Fe] > 1.0$. The stars HD 5395 and 81192 show only a slight overabundances with $[Sr/Fe] \sim 0.26$ and 0.58 respectively. For the remaining four stars the Sr abundance could not be measured as the line at 4607.327 Å appears distorted. None of the Sr II lines detected in the spectra were usable for abundance estimates.

The abundance of Y was derived for all the stars except for HD 201626. HD 16458, 125079, 216219 and 48565 show an overabundance with $[Y/Fe] > 1.0$. In the case of HD 4395, $[Y/Fe] \sim 0.65$. The remaining four stars show near-solar values.

We could derive Zr abundance for six stars. Three stars show an overabundance with $[Zr/Fe] \geq 1.0$. HD 214714 shows an underabundance with $[Zr/Fe] \sim -0.28$ and HD 81192 gives a near-solar value. HD 4395 shows overabundance with $[Zr/Fe] \sim 0.58$.

6.6 Ba, La, Ce, Pr, Nd, Sm, Eu, Dy

Standard abundance determination method using equivalent width measurements were used for the elements Ce, Pr, Nd, Sm and Dy. Spectrum synthesis calculation was carried out for Ba, La and Eu. We could determine the abundances for Ba, Ce and Nd for all the stars. The derived abundances are found to be overabundant with respect to Fe.

Barium (Ba): We have determined Ba abundances by synthesising Ba II line at 5853.668 Å considering hyperfine components from McWilliam (1998). Five of our program stars HD 125079, 216219, 16458, 48565 and 201626 show over abundance of Ba with $[Ba/Fe] \geq 1.0$. HD 4395 shows an over abundance with $[Ba/Fe] \sim 0.79$. While HD 5395, 81192 and 188650 show near solar values, HD 214714 shows mild under abundance with $[Ba/Fe] \sim -0.31$.

Lanthanum (La): We derived La abundance for HD 16458, 201626, 216219, 4395, 48565, 5395, 81192 from spectrum synthesis calculation of La II line at 4921.77 Å considering hyperfine components from Jonsell et al. (2006). Except for HD 81192 and 5395, La in all other stars is found to be overabundant relative to Fe with $[La/Fe] \geq 1$. HD 81192 and 5395 show $[La/Fe]$ of -0.13 and 0.24 respectively.

Cerium (Ce): We derived Ce abundance for all the program stars. In HD 125079 $[Ce/Fe] \sim 0.93$. While three stars

HD 188650, 214714 and 5395, show almost near-solar values, HD 16458, 201626, 216219 and 48565 give 1.47, 1.89, 1.03 and 1.42 respectively for $[\text{Ce}/\text{Fe}]$. HD 4395 give $[\text{Ce}/\text{Fe}] \sim 0.42$ and HD 81192 show a mild underabundance with $[\text{Ce}/\text{Fe}] \sim -0.15$.

Praseodymium (Pr): We could derive Pr abundance in all the program stars except for HD 81192 mainly using the Pr II line at 5292.619 Å. A mild over enhancement of Pr is seen in HD 188650 and 4395 with $[\text{Pr}/\text{Fe}] \sim 0.57$ and 0.53 respectively. In all other stars Pr shows an overabundance with values ≥ 0.79 .

Neodymium (Nd): Abundance of Nd was estimated for all the program stars. HD 188650 and 214714 show mild overabundance with $[\text{Nd}/\text{Fe}] \sim 0.39$ and 0.36 respectively. Two stars HD 4395 and 5395 give $[\text{Nd}/\text{Fe}] \sim 0.8$ and 0.74 respectively. While HD 16458, 48565, 125079, 216219 and 81192 show an overabundance with $[\text{Nd}/\text{Fe}] \geq 1.0$, HD 201626 shows a large overabundance with $[\text{Nd}/\text{Fe}] \sim 2.24$.

Samarium (Sm): Except for HD 125079, we used at least two clean lines for deriving the Sm abundance. HD 188650 shows a mild underabundance with $[\text{Sm}/\text{Fe}] \sim -0.12$. This value is found to be 0.56, 0.46, 0.85 and 0.91 respectively in HD 125079, 214714, 81192 and 216219. Abundance of Sm is derived from a single Sm II line at 4577.690 Å in HD 125079. Four objects HD 16458, 201626, 4395 and 48565 show an overabundance with $[\text{Sm}/\text{Fe}] \sim 1.87, 1.63, 1.08$ and 1.18 respectively. We could not estimate Sm abundances in HD 5395.

Europium (Eu): The abundance of Eu was derived for HD 16458 and 5395 using spectrum synthesis of Eu II lines at 6437.640 Å and 6645.130 Å by considering the hyperfine components from Worley et al. (2013). Eu shows an overabundance with $[\text{Eu}/\text{Fe}] \sim 0.67$ and 0.34 respectively. In HD 48565 we have used the Eu II line at 4129.700 Å and hyperfine components are taken from Mucciarelli et al. (2008). Eu is found to be slightly overabundant with $[\text{Eu}/\text{Fe}] \sim 0.29$. In case of HD 216219 we note that the above Eu II lines are marginally asymmetric on the right wings. These lines however, return a near solar value with $[\text{Eu}/\text{Fe}] \sim 0.07$ for this object.

Dysprosium (Dy): We could derive Dy abundance for three objects HD 201626, 5395 and 81192 using the Dy II lines at 4103.310 Å and 4923.167 Å. Dy shows an overabundance in these objects with $[\text{Dy}/\text{Fe}] \geq 1.0$.

7 DISCUSSION ON INDIVIDUAL STARS

Comparisons of our estimated atmospheric parameters and elemental abundance ratios with literature values whenever available, are presented in Tables 10 and 11 respectively. In the case of HD 201626 the author gave absolute abundances ($\log(\epsilon)$), rather than abundance ratios; in Table 11, calculated abundance ratios are presented using solar Fe values from Asplund et al. (2005).

Information on the circumstellar environment of these objects are not available in the literature. Information on polarization estimates is limited to only two objects in this sample, i.e. HD 81192 and 125079. Estimated percentage polarization in B, V, R, I bands are found to be low with < 0.2 per cent in all the four bands for HD 81192 and

< 0.4 per cent for HD 125079 (Goswami & Karinkuzhi 2013).

HD 125079, 4395, 216219: These three low-velocity CH stars are identified as CH sub-giants by Bond (1974). Spectral characteristics of sub-giant CH stars are similar to giant CH stars. With lower temperatures and luminosities the CH sub-giants occupy a position below the giants in H-R diagram. High resolution spectroscopic analyses of sub-giant CH stars by Sneden & Bond (1976) and Luck & Bond (1982) have confirmed in this type of objects the enhancement of heavy elements and a metal deficiency in the range -0.2 to -0.5. As in the case of CH giants, abundance peculiarities of sub-giant CH stars are also explained as due to mass transfer mechanisms from their binary companions (Luck & Bond 1991). Smith et al. (1993) have reported the abundances for elements Y, Zr, Ba and Nd. The effective temperature adopted by us is about 250 K larger than what they have considered for these three stars. The estimated metallicity values are about 0.15 dex lower than their estimates. For HD 125079, our estimated abundances for Y is about 0.3 dex higher and for Ba and Nd, the values are about 0.2 dex higher. In addition, we have also estimated the abundances of Ce, Pr and Sm in these objects. For the other two stars we have derived almost similar abundances for Y. For Zr, Ba and Nd, our estimated abundances are slightly higher than their values.

HD 16458: This star is included both in the Ba star catalogue of Lü (1991) and CH star catalogue of Bartkevičius (1996). Estimated radial velocity is about 18.24 km s⁻¹. Chemical composition studies of this object with respect to the abundances of a standard giant star β Gem by Tomkin & Lambert (1983) have suggested enhancement of heavy elements in this object. Smith (1984) also studied this star and reported the enhancement of heavy elements. Our abundance estimates are slightly higher compared to Smith (1984). With $[\text{Ba}/\text{Fe}]$ value ~ 1.18 and $[\text{Ba}/\text{Eu}] \sim 0.50$ this star satisfies the conditions for CEMP-r/s stars (Beers & Christlieb 2005). Long-term radial velocity monitoring of HD 16458 by McClure & Woodsworth (1990) have confirmed it to be a binary star.

HD 5395: HD 5395 is also included both in the Ba star catalogue of Lü (1991) and CH star catalogue of Bartkevičius (1996). McWilliam (1990) provided the elemental abundances for Sr, Zr, Y, La and Nd. We present updates on these abundances along with the first estimates of abundances for Ba, Ce, Pr and Eu. While Y, Ba and Ce show almost near-solar values, Sr and La show mild enhancement with $[\text{Sr}/\text{Fe}] = 0.26$ and $[\text{La}/\text{Fe}] = 0.24$. Pr, Nd and Eu show larger enhancement with respect to Fe. As far as the chemical abundances are concerned this object does not seem to belong to the group of CH stars if we stick to the definition that CH stars are those that show high abundance of s-process elements with $[\text{Ba}/\text{Fe}] > 1$.

HD 214714 and 188650: The spectra of HD 214714 and 188650 show a close resemblance. Bidelman (1957) first noticed strong bands of CH and moderate CN bands in the spectra of these stars and called them as low-velocity CH stars. Our estimated radial velocities for these two objects are -7.04 and -24.6 km s⁻¹ respectively. Strong ionised lines of elements seen in their spectra indicate high luminosity. However, following Morgan, Keenan & Kellman (1943), Luck (1991) referred to these objects as a cyanogen weak

Table 6: Elemental abundances

Star Name	[Na I/Fe]	[Mg I/Fe]	[Ca I/Fe]	[Sc II/Fe]	[Ti I/Fe]	[Ti II/Fe]	[V I/Fe]	[Cr I/Fe]	[Cr II/Fe]	[Mn I/Fe]	[Co I/Fe]	[Ni I/Fe]	[Zn I/Fe]
Subgiant-CH stars													
HD 4395	0.23	0.12	0.01	-0.09	0.04	0.22	-0.14	0.01	0.15	-0.23	-0.19	-0.02	0.18
HD 125079	0.34	0.05	0.03	0.02	0.0	0.45	-0.12	-0.06	-	-0.22	0.03	0.07	0.11
HD 216219	0.32	0.15	0.14	-0.18	0.11	0.29	-0.13	-0.09	0.12	-0.32	0.03	0.00	0.16
# CH stars													
* HD 5395	-0.39	0.12	0.04	0.04	0.08	0.18	-0.24	-0.19	0.0	-0.5	0.20	-0.09	0.29
* HD 16458	0.65	0.04	0.28	0.10	0.31	0.41	0.25	0.29	-	0.06	0.49	0.15	0.43
* HD 48565	0.18	0.15	0.11	-0.11	0.04	0.30	-0.21	-0.19	-0.32	-0.42	-0.15	-0.17	-0.18
HD 81192	-0.29	0.29	0.18	0.25	0.25	0.25	0.10	-0.33	-0.23	-0.40	0.28	0.08	-0.14
HD 188650	0.76	0.27	-0.02	-0.49	0.24	0.24	-0.24	-0.04	0.01	-0.24	0.06	-0.16	-0.05
HD 214714	0.47	0.0	0.17	-0.54	-0.19	0.32	-0.44	-0.32	-0.23	-0.49	-0.06	-0.26	-0.13
HD 201626	0.41	0.69	0.65	0.04	0.74	0.81	-	-0.59	-	-	0.00	-0.11	-0.04

Objects from the CH star catalogue of Bartkevicius (1996)
 * Objects are also included in Ba star catalogue of Lü (1991)

Table 6: continued

Star Name	[Sr I/Fe]	[Y II/Fe]	[Zr II/Fe]	[Ba II/Fe]	[La II/Fe]	[Ce II/Fe]	[Pr II/Fe]	[Nd II/Fe]	[Sm II/Fe]	[Eu II/Fe]	[Dy II/Fe]
Subgiant-CH stars											
HD 4395	1.08	0.65	0.58	0.79	1.03	0.42	0.53	0.80	1.08	-	-
HD 125079	1.59	1.05	-	1.06	-	0.93	1.00	1.16	0.56	-	-
HD 216219	1.8	1.00	0.98	1.10	1.04	1.03	1.14	0.99	0.91	0.07	-
# CH stars											
* HD 5395	0.26	0.05	-	0.03	0.24	0.06	0.79	0.74	-	0.34	1.38
* HD 16458	1.37	1.46	1.17	1.18	1.42	1.47	1.82	1.55	1.87	0.66	-
* HD 48565	1.73	1.08	0.9	1.52	1.46	1.42	1.29	1.51	1.18	0.29	-
HD 81192	0.58	0.10	0.12	0.13	-0.13	-0.15	-	1.01	0.85	-	1.21
HD 188650	-	-0.03	-	-0.01	-	-0.03	0.57	0.39	-0.12	-	-
HD 214714	-	0.22	-0.28	-0.31	-	0.05	0.93	0.36	0.46	-	-
HD 201626	-	-	-	2.12	1.76	1.89	2.09	2.24	1.63	-	0.97

Objects from the CH star catalogue of Bartkevicius (1996)
 * Objects are also included in Ba star catalogue of Lü (1991)

giants as their spectrum is characterised by weak violet CN bands. Using a curve of growth method in comparison with β Aqr, Baird et al. (1975) estimated chemical abundances for these objects and reported a high lithium abundance for HD 214714. Our chemical analysis with respect to solar values indicates a mild enhancement of heavy elements. We present first-time estimates of chemical abundances for HD 188650 based on high-resolution spectrum. The abundance of Eu could not be estimated for this object. Light s-process element Y, and heavy s-process elements Ba, Ce and Sm show near-solar values in this object. Pr and Nd also show mild enhancement with $[\text{Pr}/\text{Fe}] \sim 0.57$ and $[\text{Nd}/\text{Fe}] \sim 0.39$ respectively. This object does not seem to represent the characteristic properties of CH stars as far as the heavy element abundances are concerned.

HD 201626 : This object was first identified as a CH star by Wallerstein & Greenstein (1964); its spectrum closely resembles the spectrum of the well-known CH star HD 26. This is a high velocity object with a radial velocity of -141.6 km s^{-1} and metallicity $[\text{Fe}/\text{H}] \sim -1.4$. Abundances of heavy elements Ba, La, Ce, Pr, Nd, Sm and Dy with respect to Fe are found to be highly enhanced in this object. Our estimates of heavy element abundances are in good agreement with the estimates of Vanture (1992c)

HD 48565: The object HD 48565 is known to show abnormally strong Sr line at 4077 \AA (North et al. 1994). Bidelmann (1981) classified these type of objects as F Str λ 4077 stars. They exhibit enhancement of light and heavy s-process elements but abundances of iron-peak elements are similar to those generally seen in F type stars. Allen & Barbay (2006a) have given the abundance estimates for heavy elements in this star. Our results are slightly higher than their results, with $[\text{X}/\text{Fe}]$ values > 1 for all the heavy elements (Table 11). Our estimated radial velocity (-25.74 km s^{-1}) is about 6 km/s lower than the literature value. This object is showing a large radial velocity variations (North

et al. (1994), Nordström et al. (2004)) giving indications of the object being a binary system.

HD 81192: Except for Sr, Nd and Sm this object shows almost near-solar values for Y, Zr, Ba, La, and Ce with respect to Fe. Morgan, Keenan & Kellman (1943) have noted weaker CN bands in HD 81192 compared to other stars of same temperature and luminosity. Weakening of CN band is most common in stars with high space velocities. **Estimated** radial velocity of this object is 136 km s^{-1} . Cottrell et al. (1986) have studied the kinematics and elemental abundances of this object. Estimated heavy element abundances by Luck & Bond (1985) are found to be in close agreement with our estimates. We present first-time estimates of abundances for Sr, Sm and Dy for this object. With $[\text{Ba}/\text{Fe}] = 0.13$, this object too does not seem to belong to the group of CH stars.

7.1 Stellar masses

We derived the mass of the program stars from their locations in the Hertzsprung-Russel diagram (Figures 8 to 10), using Girardi et al. (2000) database of evolutionary tracks in the mass range of $0.15 M_{\odot}$ to $7.0 M_{\odot}$ and the Z values from 0.0004 to 0.03. These evolutionary tracks are available at <http://pleiadi.pd.astro.it/>. Since $[\text{Fe}/\text{H}]$ of our target stars are near solar, we have selected an initial composition of $Z=0.0198$, $Y=0.273$. The masses derived using spectroscopic temperature estimates are presented in Table 12. For four stars in our sample that have metallicities < -0.5 we also used evolutionary tracks for $Z = 0.008$, but the masses obtained are found to be similar to those obtained using evolutionary tracks with $Z = 0.019$. Derived stellar masses are in general $< 2 M_{\odot}$, except for HD 188650 and 214714, for which our estimated stellar masses are 3.5 and $4 M_{\odot}$ respectively.

Table 7: Observed values for [Fe/H], [ls/Fe], [hs/Fe] and [hs/ls]

Star Name	[Fe/H]	[ls/Fe]	[hs/Fe]	[hs/ls]	Remarks
HD 4395	-0.18	0.77	0.82	0.05	1
	-0.33	0.7	0.5	-0.2	2
HD 5395	-0.24	0.16	0.27	0.11	1
HD 16458	-0.65	1.34	1.50	0.16	1
HD 48565	-0.59	1.24	1.47	0.23	1
HD 81192	-0.50	0.26	0.34	0.08	1
HD 125079	-0.18	1.32	0.93	-0.39	1
HD 188650	-0.45	-0.03	0.23	0.26	1
HD 201626	-1.39	-	1.93	-	1
	-1.3	1.1	1.6	0.5	2
HD 214714	-0.35	-0.03	0.14	0.17	1
HD 216219	-0.17	1.26	1.01	-0.25	1
	-0.32	1.0	0.9	-0.1	2

1. Our work; 2: Busso et al. (2001)

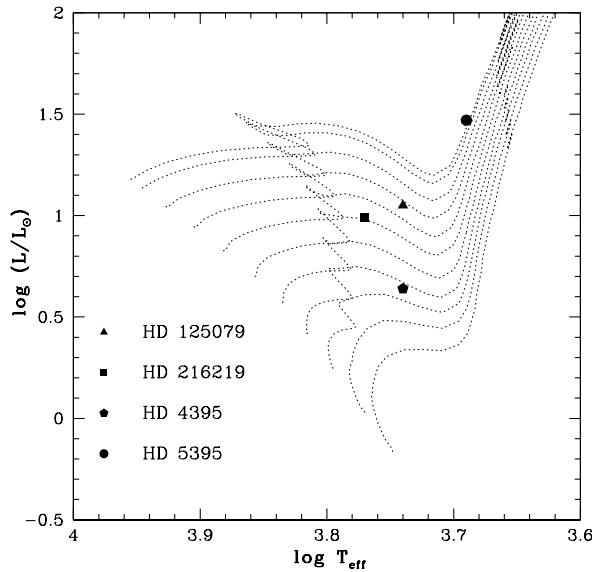


Figure 8. The location of HD 125079, HD 216219, HD 4395 and HD 5395 are indicated in the H-R diagram. The masses are derived using the evolutionary tracks of Girardi et al. (2000). The evolutionary tracks for masses 1, 1.1, 1.2, 1.3 1.4, 1.5, 1.6 1.7, 1.8, 1.9 and 1.95 M_{\odot} from bottom to top are shown in the Figure.

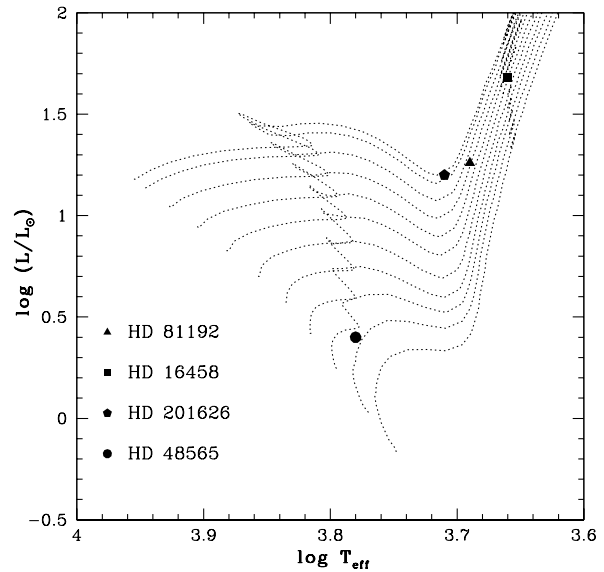


Figure 9. The location of HD 81192, HD 16458, HD 201626 and HD 48565 are indicated in the H-R diagram. The masses are derived using the evolutionary tracks of Girardi et al. (2000). The evolutionary tracks are shown for masses 1, 1.1, 1.2, 1.3 1.4, 1.5, 1.6 1.7, 1.8, 1.9 and 1.95 M_{\odot} from bottom to top.

8 PARAMETRIC MODEL BASED STUDY

Elements heavier than iron are produced mainly by two neutron-capture processes, the s-process and the r-process. Observed abundances of heavy elements estimated using model atmospheres and spectral synthesis techniques do not provide direct quantitative estimates of the relative contributions from s- and/or r- process nucleosynthesis. We investigated ways to delineate the observed abundances into their

respective r- and s-process contributions in the framework of a parametric model using an appropriate model function. The origin of the n-capture elements is explored by comparing the observed abundances with predicted s- and r-process contributions following Goswami et al. (2010a, and references there in). Identification of the dominant processes contributing to the heavy element abundances in CEMP stars is likely to provide clues to the origin of the observed

Table 8: Equivalent widths (in mÅ) of lines used for the calculation of light element abundances

Wavelength	Element	E_{low}	log gf	HD 4395	HD 5395	HD 16458	HD 48565	HD 81192	HD 125079	HD 188650	HD 201626	HD 214714	HD 216219
5682.650	Na I	2.100	-0.700	94.6	-	143.4	48.66	-	109.7	109.9	-	95.46	81.17
5688.220		2.100	-0.400	100.6	-	149.9	-	-	120.9	138.2	-	128.4	107.1
5889.950		0.000	0.100	-	411.5	-	-	411.5	-	-	-	-	358.0
5895.920		0.000	-0.200	347.2	378.6	536.7	242.5	378.6	-	-	214.0	-	284.4
4702.990	Mg I	4.350	-0.666	-	-	238.8	150.3	202.1	199.9	174.9	133.2	174.9	178.8
6318.720		5.108	-1.730	-	52.21	52.79	15.55	-	-	-	-	26.95	-
5528.400		4.350	-0.490	185.7	211.8	192.4	143.5	211.8	199.5	184.9	-	176.2	157.2
4098.520	Ca I	2.525	-0.540	-	-	-	47.8	-	-	66.2	63.5	95.4	85.3
4283.010		1.885	-0.224	-	-	-	109.8	-	-	-	-	-	149.9
4425.430		1.879	-0.385	136.8	-	102.2	99.6	144.0	-	132.1	-	-	114.5
4435.679		1.890	-0.520	133.6	-	-	109.5	141.0	-	-	-	137.3	122.1
4455.890		1.900	-0.510	137.6	-	-	104.3	137.7	165.7	132.9	107.8	113.2	133.7
4578.550		2.521	-0.560	64.2	-	-	47.19	102.6	98.7	47.52	-	-	67.2
5261.710		2.521	-0.730	90.9	112.4	146.6	55.70	-	102.7	80.50	52.2	92.9	79.5
5265.560		2.520	-0.110	-	-	-	-	-	-	160.	5	-	-
5512.990		2.932	-0.290	76.5	-	135.3	45.36	87.4	86.2	54.8	-	-	68.1
5581.980		2.523	-0.710	89.1	-	125.7	58.81	115.6	107.2	79.45	-	93.9	84.51
5588.760		2.530	0.360	129.7	-	-	102.8	140.9	141.8	137.4	-	137.5	127.7
5590.130		2.521	-0.710	82.7	-	94.4	54.1	103.2	94.0	-	-	86.08	77.9
5594.470		2.520	0.100	108.9	-	-	-	-	156.0	-	164.6	-	-
5857.450		2.930	0.240	120.8	-	170.3	82.3	131.4	137.5	130.9	-	-	111.0
6162.170		1.900	-0.090	-	210.5	-	-	200.9	204.8	187.3	132.0	185.2	162.9
6439.070		2.530	0.390	141.8	168.0	185.2	106.8	161.3	162.8	162.6	-	161.8	140.0
6449.820		2.520	-0.550	78.5	-	-	60.7	-	-	-	-	118.8	88.7
6455.590		2.523	-1.350	53.9	-	111.0	-	79.7	-	-	-	-	45.5
6471.670		2.525	-0.590	93.7	-	134.8	52.3	-	98.8	81.1	54.5	86.4	79.6
6493.790		2.521	0.140	145.8	-	168.4	88.1	136.8	130.6	111.4	-	127.0	111.9
6499.650		2.523	-0.590	79.7	-	-	44.3	-	95.9	55.5	-	-	75.1
6717.690		2.709	-0.610	-	-	186.0	60.7	-	-	-	-	105.6	95.9
4431.110	Sc II	6.035	-2.520	-	-	25.0	-	-	-	-	68.3	-	-
4400.389		0.606	-0.510	-	-	-	-	-	-	-	-	158.5	-
5031.021		1.360	-0.260	79.5	-	-	61.9	-	119.3	131.7	-	-	-
6604.600		1.357	-1.480	-	-	-	22.7	-	60.41	-	-	65.85	-
6245.637		1.507	-1.030	-	73.1	74.5	21.7	61.4	56.9	69.3	34.3	72.7	46.9
4512.700	Ti I	0.836	-0.480	64.9	-	115.3	34.9	79.1	82.9	48.3	-	56.7	53.7
4453.710		1.873	-0.010	52.9	-	-	18.1	66.57	-	-	-	-	-
4533.239		0.848	0.476	111.6	-	-	71.4	140.1	-	-	73.6	-	99.25
4617.250		1.748	0.389	-	88.4	-	29.3	83.5	-	35.31	-	-	-
4656.468		0.000	-1.345	56.2	-	150.1	30.4	104.7	85.8	37.8	-	46.8	-
4759.272		2.255	0.514	-	76.7	-	18.3	63.9	59.7	16.4	-	26.4	39.2
4820.410		1.502	-0.441	-	89.2	-	-	86.5	-	23.6	64.5	36.9	62.7
4840.880		0.899	-0.509	-	-	119.3	26.9	86.4	79.4	-	-	-	52.7
4778.250		2.236	-0.220	-	34.3	71.7	-	-	19.6	-	-	-	-
4999.500		0.830	0.310	101.0	-	-	-	136.7	-	-	-	131.2	-
4937.730		0.813	-2.230	117.1	35.1	74.1	-	-	-	-	-	-	-
5007.210		0.820	0.170	-	-	-	-	152.3	-	-	108.8	-	-
5039.960		0.020	-1.130	-	124.6	-	42.8	-	105.3	66.9	-	83.4	72.9
5064.650		0.050	-0.940	94.0	145.3	-	42.8	-	-	-	-	-	68.9
5087.060		1.429	-0.780	-	80.2	93.8	-	92.8	-	-	-	-	-
5210.390		0.048	-0.884	-	127.5	-	52.7	-	111.4	81.2	-	97.3	78.2
6556.060		1.460	-1.074	93.1	60.7	104.0	-	-	33.72	-	-	-	-
4161.530	Ti II	1.080	-2.160	66.2	-	-	-	-	-	-	-	108.1	-
4417.710		1.160	-1.430	-	-	-	-	-	141.8	-	-	160.8	117.5
4418.330		1.240	-1.990	-	-	140.0	67.5	98.3	-	-	-	112.7	83.42
4443.790		1.080	-0.700	138.1	175.3	179.7	123.4	124.6	181.5	196.8	128.6	-	145.3
4468.520		1.130	-0.600	-	-	-	-	-	186.8	-	-	-	-
4470.900		1.164	-2.280	-	88.9	-	53.8	-	-	115.7	71.01	-	75.79
4493.510		1.080	-2.730	-	-	84.4	32.04	52.10	-	62.26	60.59	79.18	60.06
4563.760		1.221	-0.960	131.2	-	210.7	110.4	150.6	-	-	121.9	193.6	141.6
4571.960		1.571	-0.530	139.1	-	-	118.5	-	-	-	68.33	-	165.1
4568.310		1.224	-2.650	-	-	94.1	-	66.1	-	56.8	15.3	-	35.8
4657.210		1.240	-2.320	51.7	-	47.41	46.81	64.6	-	-	-	-	-
4708.665		1.240	-2.370	-	83.6	-	-	-	-	-	-	-	66.7
4798.510		1.080	-2.670	-	-	-	32.8	-	-	-	-	-	65.8
4805.090		2.060	-1.100	101.1	-	134.3	75.2	108.5	-	154.6	100.8	147.1	108.2
5185.900		1.890	-1.350	-	-	-	88.3	-	-	63.9	126.3	-	69.8
5226.530		1.570	-1.300	-	141.9	165.2	83.7	107.8	-	-	96.5	-	110.1
4090.570	V I	1.853	-2.099	-	-	-	-	-	-	-	96.4	-	-
4379.230		0.300	0.580	119.3	-	215.3	57.40	110.8	124.3	84.8	-	-	87.3
4406.630		0.300	-0.190	-	-	220.7	47.2	122.9	-	73.4	-	-	68.1
4876.430		2.115	-2.714	-	-	-	-	-	-	-	-	99.8	-
5727.653		1.051	-0.870	-	95.0	76.3	45.0	37.1	17.2	-	-	-	-
6531.420		1.218	-0.840	-	-	51.1	-	-	-	-	-	-	-
4274.800	Cr I	0.000	-0.230	200.8	-	-	147.4	-	-	-	-	-	161.6
4289.720		0.000	-0.360	-	-	-	86.5	-	-	-	88.4	-	-
4351.050		0.970	-1.450	55.1	-	-	-	48.6	-	-	-	-	45.31
4600.750		1.000	-1.260	-	-	-	-	-	-	-	-	-	47.8
4616.140		0.980	-1.190	87.4	115.9	202.5	54.7	-	110.1	99.9	32.8	116.4	74.0
4626.190		0.970	-1.320	80.9	106.9	111.6	43.8	94.8	97.7	86.3	-	100.9	62.25
4652.160		1.000	-1.030	103.1	-	184.1	57.6	113.2	122.2	110.8	-	117.4	94.59
4737.380		3.087	-0.099	59.9	75.8	109.8	-	-	-	24.3	-	-	68.6
4942.490		0.941	-2.294	-	-	163.5	29.2	-	-	64.8	-	72.1	-
5206.040		0.940	0.020	-	-	-	-	-	-	-	-	-	169.3
5247.570		0.961	-1.640	77.4	-	140.5	34.3	84.7	-	77.2	-	89.1	641
5345.810		1.003	-0.980	115.4	159.3	-	70.7	140.8	137.9	-	-	140.2	105.8
5348.312		1.003	-1.290	-	-	-	-	-	-	-	51.3	107.0	-

abundances. The i th element abundance can be calculated as

$$N_i(Z) = A_s N_{is} + A_r N_{ir} 10^{[Fe/H]}$$

where Z is the metallicity of the star, N_{is} indicates the abundance from s-process in AGB star, N_{ir} indicates the abundance from r-process; A_s indicates the component coefficient that correspond to contributions from the s-process and A_r indicates the component coefficient that correspond to contributions from the r-process.

We utilized the solar system s- and r-process isotopic

abundances from stellar models of Arlandini et al. (1999). The observed elemental abundances were scaled to the metallicity of the corresponding CH star and normalised to their respective Ba abundances. Elemental abundances were then fitted with the parametric model function. The best fit coefficients and reduced chi-square values for a set of CH stars are given in Table 13. The best fits obtained with the parametric model function $\log \epsilon_i = A_s N_{is} + A_r N_{ir}$ for HD 16458, 48565, 125079, and 216219 are shown in Figures 11 -14. The errors in the derived abundances play an

Table 8: Continued

Wavelength	Element	E_{low}	log gf	HD 4395	HD 5395	HD 16458	HD 48565	HD 81192	HD 125079	HD 188650	HD 201626	HD 214714	HD 216219
4588.190	Cr II	4.072	-0.630	66.6	73.5	-	57.7	49.3	-	131.1	-	99.9	84.2
4592.040		4.073	-1.220	33.2	48.6	-	33.2	27.3	-	81.9	-	64.2	52.7
4812.350	Mn I	3.864	-1.800	-	-	-	19.8	40.9	-	-	-	42.5	41.67
4634.070		4.073	-1.240	-	-	-	-	-	-	102.5	-	-	73.7
4848.250		3.864	-1.140	-	-	-	-	-	-	-	-	87.16	65.3
4030.750		0.000	-0.470	-	-	-	-	-	-	-	115.1	-	-
4034.480		0.000	-0.810	-	-	-	125.3	-	-	176.0	-	-	183.0
4041.360		2.110	0.280	-	195.2	-	102.6	-	151.3	-	68.66	-	143.0
4451.580		2.890	0.280	-	-	131.7	73.42	73.69	116.5	95.92	-	98.18	97.47
4470.140		2.941	-0.444	37.5	56.8	59.4	11.5	41.4	63.6	41.2	23.1	23.8	28.00
4739.080		2.941	-0.490	44.2	80.9	124.6	17.9	-	73.4	48.3	-	56.2	36.9
4761.530		2.953	-0.138	67.8	100.0	105.9	25.3	-	90.2	62.8	-	68.3	59.6
4765.860		2.941	-0.080	68.4	100.8	95.9	32.8	-	82.8	63.5	-	67.0	57.0
4766.420	Co I	2.919	0.100	83.0	127.8	140.7	46.38	109.6	-	95.96	23.9	-	72.52
4783.430		2.300	0.040	125.6	159.3	200.9	75.8	-	137.9	136.8	-	138.1	107.2
5516.770		2.178	-1.847	-	93.2	141.6	-	-	-	26.2	-	43.52	20.2
6013.488		3.072	-0.250	75.8	108.3	148.9	23.9	84.9	98.9	66.9	-	74.8	54.3
4813.480		3.216	0.050	-	-	-	10.57	46.3	-	24.2	-	-	-
4121.320		0.920	-0.320	125.2	-	-	-	-	-	-	-	135.3	107.9
4118.770		1.050	-0.490	-	-	-	-	-	-	-	70.1	-	-
4749.660		3.053	-0.321	-	-	-	-	74.8	-	-	-	-	-
4771.080		3.133	-0.504	-	59.0	72.4	-	-	-	-	-	-	-
4781.430		1.882	-2.150	-	33.8	73.7	-	-	-	-	-	-	-
4792.850	Ni I	3.252	-0.067	29.3	52.6	-	-	-	-	-	-	-	-
5530.770		1.710	-2.067	-	52.9	98.5	-	46.1	-	-	-	-	-
5590.720		2.042	-1.870	-	47.3	92.1	-	-	25.2	-	-	-	-
5991.870		2.080	-1.850	-	59.7	97.7	7.483	-	-	-	-	-	-
6454.990		2.632	-0.233	-	-	40.2	-	-	-	-	-	-	-
6632.430		2.280	-2.000	-	29.3	59.6	-	-	-	-	-	-	-
4470.470		3.699	-0.400	-	-	-	-	-	-	-	-	34.3	-
4714.420		3.380	0.230	-	-	-	83.4	132.7	164.4	-	-	-	126.4
4732.460		4.106	-0.550	33.18	-	-	11.5	29.5	-	-	-	-	-
4814.590		3.597	-1.680	-	-	54.4	-	16.3	49.7	-	-	-	-
4821.130	Zn I	4.153	-0.850	-	-	60.1	-	32.8	-	15.4	-	-	-
4852.560		3.542	-1.070	32.5	-	-	-	46.8	52.1	24.4	-	32.7	28.3
4855.410		3.540	0.000	84.8	-	111.1	53.2	98.9	-	-	27.5	-	-
4857.390		3.740	-1.199	44.6	-	-	13.5	60.7	60.2	27.8	-	-	34.2
4953.200		3.740	-0.670	46.9	-	-	17.8	66.7	61.6	36.9	-	38.8	35.6
4937.340		3.606	-0.390	66.6	-	120.2	36.3	-	-	62.7	-	71.8	61.9
4980.160		3.610	-0.110	94.5	-	-	57.5	92.2	-	-	40.1	92.6	87.8
5035.370		3.630	0.290	79.3	-	94.3	63.6	94.6	-	95.4	-	87.5	73.7
5081.120		3.847	0.300	84.3	102.9	97.3	58.2	81.5	92.3	83.9	-	80.6	69.57
5082.350		3.657	-0.540	62.5	76.6	-	30.0	-	75.1	42.3	-	58.9	47.3
5084.080	Zn I	3.678	0.030	74.9	94.1	77.7	51.8	75.9	90.2	72.5	-	74.1	71.5
5099.930		3.678	-0.100	80.9	-	-	46.8	-	-	-	-	96.5	73.6
5102.960		1.676	-2.620	58.7	-	-	18.2	-	-	-	-	37.0	35.4
5259.470		3.740	-1.502	10.0	-	114.3	-	-	-	-	-	-	17.8
6086.280		4.266	-0.530	35.1	51.9	64.3	11.7	33.6	45.8	23.9	-	27.2	-
6111.070		4.088	-0.785	31.6	45.5	59.1	-	30.0	36.3	-	-	-	27.4
6176.810		4.088	-0.148	-	-	93.8	23.5	-	68.6	42.0	-	-	20.3
6186.710		4.106	-0.777	-	42.2	-	-	-	33.6	-	-	-	48.2
6204.600		4.088	-1.060	-	30.7	56.9	-	-	26.7	-	-	-	-
6643.640		1.676	-2.300	94.4	145.5	169.0	41.8	118.4	-	86.8	50.9	100.9	77.7
4722.150	Zn I	4.029	-0.370	76.0	-	-	52.6	51.6	-	89.5	152.3	91.2	85.9
4810.530		4.080	-0.170	-	-	90.7	51.3	68.1	87.5	101.2	47.1	89.5	76.7

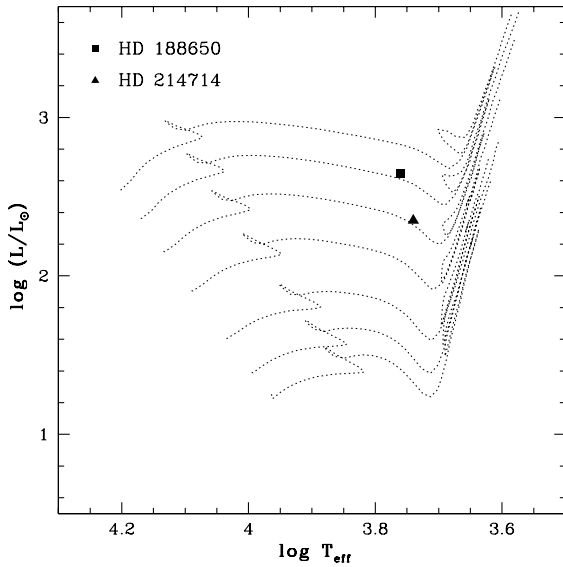


Figure 10. The location of HD 188650, and HD 214714 are indicated in the H-R diagram. The evolutionary tracks of Girardi et al. (2000) are shown for masses 2, 2.2, 2.5, 3.0, 3.5, 4.0 and 4.5 M_{\odot} from bottom to top.

important role in deciding the goodness of fit of the parametric model functions. From the parametric model based analysis we find HD 16458 to fall in the group of CEMP r/s stars and the stars HD 48565, HD 125079, and HD 216219 belong to the group of CEMP-s stars.

9 CONCLUSIONS

Elemental abundances are presented for twenty two elements for a set of ten stars from the CH star catalogue of Bartkevičius (1996). The sample includes eight low-velocity CH stars ($V_r \leq \pm 50 \text{ km s}^{-1}$) and two high-velocity ($V_r \geq \pm 100 \text{ km s}^{-1}$) CH stars. Metallicity $[\text{Fe}/\text{H}]$ of the two high-velocity stars HD 201626 and 81192 are found to be -1.4 and -0.5 respectively. The low-velocity stars metallicity ranges from -0.18 to -0.66 . While Ba abundance is measured in all the ten stars, we could measure the Eu abundance only for four stars.

Beers & Christlieb (2005) have used the Ba and the Eu abundances to classify CEMP stars into several broad categories, among which CEMP-s stars are those that exhibit large over-abundances of s-process elements with $[\text{Ba}/\text{Fe}] > +1$ and $[\text{Ba}/\text{Eu}] > +0.5$. In this classification scheme CEMP-r/s, stars are those with $0 < [\text{Ba}/\text{Eu}] < +0.5$; they exhibit both r- and s-process enhancements. CEMP-s stars are believed to be the metal-poor counterparts of CH stars having same origin as CH stars. The observed chemical com-

Table 9: Equivalent widths (in mÅ) of lines used for the calculation of heavy element abundances

Wavelength	Element	E_{low}	log gf	HD 4395	HD 5395	HD 16458	HD 48565	HD 81192	HD 125079	HD 188650	HD 201626	HD 214714	HD 216219
4607.327	Sr I	0.000	-0.570	60.4	65.6	138.6	56.5	62.9	95.9	-	-	-	80.2
4854.863	Y II	0.992	-0.380	-	77.1	-	-	63.7	-	95.3	-	-	98.1
4883.685		1.084	0.07	90.4	81.1	211.9	87.2	72.4	134.4	126.9	-	122.8	119.9
5087.416		1.080	-0.170	71.9	71.3	-	80.2	71.7	104.1	96.2	-	-	98.1
5119.112		0.992	-1.360	-	31.7	120.6	36.7	-	71.7	44.3	-	-	64.8
5205.724		1.033	-0.340	-	-	-	-	-	-	-	-	-	116.2
5289.815		1.033	-1.850	15.5	-	87.5	13.7	-	41.4	-	-	-	34.2
5544.611		1.738	-1.090	-	-	-	22.09	-	-	-	-	-	41.6
5546.009		1.748	-1.100	30.9	-	27.9	-	-	22.0	-	-	22.2	51.6
5662.925		1.944	0.160	-	-	-	63.85	-	-	-	-	-	-
6613.733		1.748	-1.11	-	42.6	119.5	22.3	-	-	-	-	-	45.5
4048.670	Zr II	0.800	-0.480	-	-	-	-	-	-	-	-	-	-
4208.990		0.710	-0.460	68.2	-	-	68.2	64.9	-	-	-	-	88.0
4317.321		0.713	-1.380	-	-	-	-	-	-	-	-	30.3	66.0
4554.036	Ba II	0.000	0.120	259.1	215.0	-	-	176.2	412.3	284.4	286.0	259.5	338.7
4130.650		2.720	+0.560	77.8	-	182.2	-	-	98.96	-	-	-	108.8
4934.076		0.000	-0.150	-	-	-	265.6	-	-	298.1	333.9	-	-
5853.668		0.604	-1.020	-	-	263.9	-	-	-	147.8	-	-	-
6141.727		0.704	-0.076	-	158.9	420.5	200.8	-	253.8	237.9	-	-	230.0
6496.897		0.604	-0.377	157.1	149.8	402.3	214.7	-	233.9	225.0	-	229.9	209.4
4123.230	La II	0.320	+0.120	-	-	-	87.1	-	-	-	-	-	-
4238.380		0.400	-0.058	92.5	68.0	-	101.1	-	-	-	-	-	97.97
4322.510		0.170	-1.050	44.3	-	-	-	19.9	-	-	-	-	-
4333.760		0.170	-0.160	108.8	-	-	-	56.6	-	-	-	-	-
4619.874		1.754	-0.140	-	-	-	22.8	-	-	-	-	-	25.7
4748.726		0.927	-0.860	-	-	72.1	23.2	-	-	-	-	-	42.1
4921.776		0.244	-0.680	67.4	85.1	173.9	64.5	72.9	-	-	78.8	-	77.9
5808.313		0.000	-2.200	-	-	77.3	-	-	-	-	-	-	-
6320.376		0.170	-1.610	-	-	-	-	-	-	-	54.4	-	-
4073.470	Ce II	0.480	+0.320	-	-	-	60.5	-	58.5	-	-	-	61.5
4117.290		0.740	-0.450	-	-	39.2	-	-	-	-	36.8	-	27.9
4190.630		0.900	-0.390	-	-	-	19.1	-	-	-	-	-	-
4193.870		0.550	-0.400	-	-	-	33.5	-	-	-	-	-	-
4257.120		0.460	-1.116	-	-	-	-	-	-	-	31.8	-	-
4336.244		0.704	-0.564	-	-	-	-	-	-	-	-	-	34.9
4418.790		0.860	+0.310	-	-	-	-	-	28.8	-	-	30.6	55.3
4427.920		0.540	-0.380	-	-	-	-	-	-	-	-	22.1	39.7
4460.207		0.477	0.171	-	-	-	-	-	-	94.8	-	-	-
4560.280		0.910	0.000	-	-	-	52.2	-	-	-	-	-	-
4562.359		0.478	0.081	-	-	132.0	60.6	34.1	74.9	48.6	78.6	69.8	73.3
4628.160		0.520	+0.260	-	46.3	135.4	64.5	-	-	44.4	-	-	76.08
4747.167		0.320	-1.246	-	-	-	14.3	-	-	-	-	-	-
4773.941		0.924	-0.498	-	24.7	20.5	-	34.9	-	47.4	12.3	30.5	-
4873.999		1.107	-0.892	-	-	57.4	-	-	-	-	-	-	-
5274.230		1.044	0.323	25.3	23.6	-	37.0	-	-	-	-	23.9	45.2
5330.556		0.869	-0.760	12.7	-	-	22.4	-	-	-	48.9	12.4	28.2
5188.217	Pr II	0.922	-1.145	-	-	34.1	-	-	-	-	-	-	-
5259.740		0.630	-0.070	10.4	-	104.6	15.1	-	-	-	-	-	-
5219.045		0.795	-0.240	-	-	92.5	-	-	-	-	-	-	17.3
5292.619		0.648	-0.300	-	42.6	104.0	15.0	-	-	16.9	-	21.4	22.8
5322.772		0.482	-0.315	-	-	109.6	12.4	-	26.1	-	54.5	-	-
5892.251		1.439	-0.352	-	-	41.8	11.1	-	-	-	-	-	-
6278.676		1.196	-0.630	-	63.8	-	-	-	-	-	-	-	-
4021.327	Nd II	0.320	0.230	-	-	-	61.8	-	-	-	-	-	-
4059.951		0.205	-0.360	-	-	60.3	-	-	-	-	-	-	31.2
4061.080		0.471	0.550	64.0	56.6	123.2	67.1	-	-	-	-	-	-
4069.270		0.060	-0.400	-	-	-	-	-	-	-	-	-	35.4
4109.448		0.320	+0.180	-	-	111.4	-	-	-	-	-	-	-
4446.390		0.200	-0.630	37.4	-	175.0	49.2	60.4	-	32.1	-	47.1	44.5
4451.563		0.381	-0.040	-	-	-	74.1	-	-	-	104.9	-	-
4451.980		0.000	-1.340	-	-	153.2	31.7	-	-	-	-	36.4	44.6
4556.133		0.064	-1.610	-	-	119.0	-	-	-	-	60.5	-	-
4797.153		0.559	-0.950	-	-	94.0	19.9	-	-	-	-	-	27.9
4811.342		0.063	-1.140	27.8	44.2	124.4	38.8	-	57.4	26.6	68.5	28.0	42.8
5089.832		0.204	-1.160	-	-	-	14.9	-	-	-	-	-	16.7
5130.590		1.300	+0.100	-	-	-	39.3	-	-	-	-	-	60.9
4859.039		0.320	-0.830	-	-	147.6	-	-	-	44.5	-	51.91	-
4947.020		0.559	-1.250	-	-	68.1	-	-	-	-	-	-	-
4961.387		0.630	-0.710	-	19.9	113.3	-	-	42.3	-	72.5	-	-
4989.953		0.680	-1.400	-	-	144.9	-	-	-	-	-	-	-
5212.361		0.204	-0.870	-	52.1	138.7	-	-	-	-	-	22.7	36.2
5293.169		0.823	-0.060	39.0	-	-	-	-	-	-	-	46.8	60.2
5276.878		0.859	-0.440	-	-	93.0	-	-	-	-	-	-	-
5287.133		0.745	-1.300	-	14.9	71.6	-	-	-	-	-	-	-
5311.480		0.990	-0.560	-	-	117.8	18.2	-	-	-	47.8	-	-
5319.820		0.550	-0.210	35.8	-	-	46.1	-	-	-	76.9	51.5	59.3
5356.967		1.264	-0.250	-	-	81.5	-	-	-	-	-	-	-
5361.510		0.68	-0.400	-	-	-	-	-	-	35.2	61.4	49.9	-
5371.927		1.412	0.003	-	-	-	-	-	-	-	-	-	30.1
5603.648		0.380	-1.830	-	-	111.5	-	-	44.7	13.8	-	-	-
5718.118		1.410	-0.340	-	-	68.1	-	-	-	-	-	-	-
5825.857		1.081	-0.760	-	-	74.9	-	-	-	-	-	-	-
4318.927	Sm II	0.280	-0.270	-	-	151.6	-	37.7	-	-	53.0	-	-
4424.337		0.485	-0.260	-	-	-	-	-	-	-	70.0	-	-
4434.318		0.378	-0.576	53.5	-	116.9	-	60.4	-	26.1	-	-	52.8
4499.475		0.248	-1.413	-	-	71.9	10.8	-	-	-	28.9	-	-
4519.630		0.540	-0.430	20.2	-	-	28.3	-	-	-	-	-	37.5
4577.690		0.250	-0.770	-	-	-	-	22.7	36.4	-	-	-	-
4566.210		0.330	-1.245	13.8	-	-	-	-	-	-	44.4	-	16.7
4674.600		0.180	-0.560	-	-	-	27.4	-	-	27.9	-	-	37.7
4704.400		0.000	-1.562	30.2	-	-	-	33.1	-	-	-	23.8	32.8
4615.444		0.544	-1.262	-	-	-	-	-	-	-	18.7	-	-
4726.026		0.333	-1.849	-	-	-	-	-	-	-	29.8	-	-
4791.580		0.104	-1.846	-	-	77.5	-	-	-	-	24.0	-	-
4815.805		0.185	-1.501	-	-	-	-	-	-	-	-	16.2	-
4129.700	Eu II	0.000	+0.204	-	-	-	74.9	-	-	-	-	-	80.3
4205.050		0.000	+0.117	-	-	-	-	-	-	-	-	-	97.2
6437.640		1.319	-0.276	-	14.8	27.3	-	-	-	-	-	-	-
6645.130		1.380	+0.204	-	-	61.9	-	-	-	-	-	-	-
4103.310	Dy II	0.103	-0.346	-	-	-	-	68.9	-	-	46.7	-	-
4923.167		0.103	-2.384	-	26.1	-	-	-	-	-	-	-	-

Table 10. Atmospheric parameters from literature

Star name	Vmag	Teff	log g	[Fe/H]	Reference
HD4395	7.50	5550	3.66	-0.17	1
		5478	3.40	-0.31	8
		5478	3.30	-0.38	2
		5450	3.30	-0.33	3
		5467	3.32	-0.35	9
HD5395	4.63	4860	2.51	-0.24	1
		4800	2.20	-1.00	6
		4770	2.90	-0.51	11
		4764	2.36	-0.44	9
HD16458	5.78	4550	1.8	-0.65	1
		4582	2.00	-0.32	4
		4582	2.00	-0.43	4
		4800	1.80	-0.30	5
		4500	1.40	-0.36	6
HD48565	7.07	6030	3.80	-0.59	1
		5910	4.27	-0.56	8
HD 81192	6.54	4870	2.75	-0.50	1
				-0.61	12
		4755	2.40	-0.60	13
		4582	2.75	-0.70	14
HD125079	8.60	5520	3.30	-0.18	1
		5305	3.50	-0.30	2
		5300	3.50	-0.16	3
HD188650	5.76	5700	2.15	-0.46	1
HD214714	6.03	5550	2.41	-0.36	1
		5400	2.38	-0.36	7
HD216219	7.40	5950	3.5	-0.17	1
		5478	2.80	-0.55	8
		5600	3.25	-0.39	2
		5600	3.20	-0.32	3
HD 201626	8.13	5120		-1.39	1

References.1. Our work 2. Smith & Lambert 1986, 3. Smith et al. 1993, 4. Tomkin & Lambert 1983, 5. Smith 1984, 6. Villacanas et al. 1990, 7. Luck 1991, 8. Krishnaswamy & Sneden 1985, 9. Soubiran et al. 2008, 10. North et al. 1994, 11. McWilliam 1990, 12. Luck & Bond 1983, 13. Luck & Bond 1985, 14. Cottrell & Sneden 1986

Table 11. Elemental Abundances from literature

Star Name	[Sr I/Fe]	[Y II/Fe]	[Zr II/Fe]	[Ba II/Fe]	[La II/Fe]	[Ce II/Fe]	[Pr II/Fe]	[Nd II/Fe]	[Sm II/Fe]	[Eu II/Fe]	[Dy II/Fe]	reference
Subgiant-CH stars												
HD 4395	1.08	0.65	0.58	0.79	1.03	0.42	0.53	0.80	1.08	-	-	1
	-	0.70	0.61	0.53	-	-	-	0.39	-	-	-	2
	1.08	0.10	1.01	-0.20	-	-	-	-0.20	-	-0.55	-	3
HD 125079	1.59	1.05	-	1.06	-	0.93	1.00	1.16	0.56	-	-	1
	-	1.36	0.98	0.89	-	-	-	0.99	-	-	-	2
HD 216219	1.80	1.00	0.98	1.10	1.04	1.03	1.14	0.99	0.91	0.07	-	1
	-	1.10	0.85	0.87	-	0.95	-	-	-	-	-	2
	1.30	0.96	-	-	0.72	0.70	-	0.83	0.53	-	-	3
CH stars												
HD 5395	0.26	0.05	-	0.03	0.24	0.06	0.79	0.74	-	0.34	1.38	1
	1.44	0.27	-1.04	-	0.17	-	-	0.38	-	-	-	4
HD 16458	1.37	1.46	1.17	1.18	1.42	1.47	1.82	1.55	1.87	0.66	-	1
	1.25	1.06	0.95	1.03	0.96	0.89	0.68	0.97	-	0.35	-	5
HD 48565	1.73	1.08	0.9	1.52	1.46	1.42	1.29	1.51	1.18	0.29	-	1
	0.97	1.01	1.19	1.29	1.39	1.60	1.09	1.31	0.95	0.35	-	6
HD 81192	0.58	0.10	0.12	0.13	-0.13	-0.15	-	1.01	0.85	-	1.21	1
	-	-0.07	-0.34	-0.12	-0.51	-0.04	-	-	-	-	-	7
HD 188650	-	-0.03	-	-0.01	-	-0.03	0.57	0.39	-0.12	-	-	1
HD 214714	-	0.22	-0.28	-0.31	-	0.05	0.93	0.36	0.46	-	-	1
	-	0.24	0.72	-	-	0.36	-	-	-	-	-	8
HD 201626	-	-	-	2.12	1.76	1.89	2.09	2.24	1.63	-	0.97	1
	-	0.09	-	-	1.6	1.62	2.09	1.55	1.6	-	-	9

References.1. Our work 2. Smith et al. (1993) 3. Luck & Bond (1982) 4. McWilliam (1990) 5. Smith (1984) 6. Allen & Barbuy (2006a) 7. Luck & Bond (1985) 8. Luck (1990) 9. Vanture (1992c)

Table 12: Stellar Masses

Star Name.	M_v	$\log(L/L_\odot)$	$Mass(M_\odot)$
HD 4395	2.8	0.64	1.35
HD 5395	0.7	1.47	1.95
HD 16458	0.1	1.68	1.5
HD 48565	3.7	0.4	1.15
HD 81192	1.2	1.26	1.7
HD 125079	1.8	1.05	1.75
HD 188650	-2.7	2.65	4.0
HD 201626	1.3	1.2	1.9
HD 214714	-1.3	2.35	3.5
HD 216219	2.1	0.99	1.6

Table 13: Best fit coefficients and reduced chi-square values

Star Name	A_s	A_r	χ^2
HD 16458	0.49 ± 0.09	0.60 ± 0.09	1.6
HD 48565	0.835 ± 0.09	0.112 ± 0.08	1.15
HD 125079	0.832 ± 0.16	0.182 ± 0.15	0.50
HD 216219	0.859 ± 0.14	0.169 ± 0.13	1.22

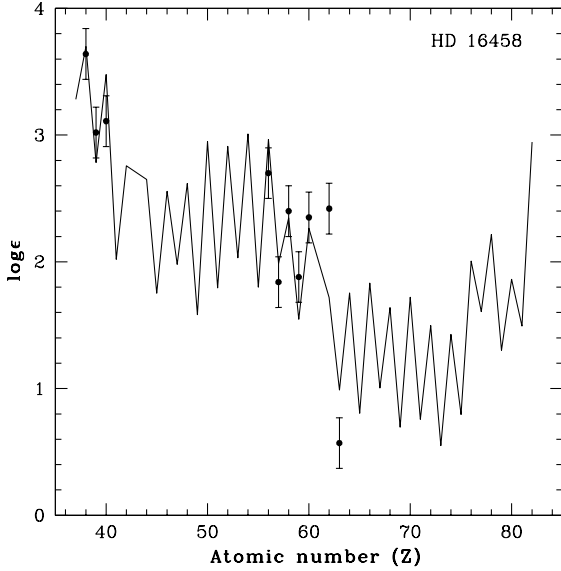


Figure 11. Solid curve represent the best fit for the parametric model function $\log \epsilon = A_s N_{si} + A_r N_{ri}$, where N_{si} and N_{ri} represent the abundances due to s- and r-process respectively (Arlandini et al. 1999, Stellar model, scaled to the metallicity of the star). The points with errorbars indicate the observed abundances in HD 16458.

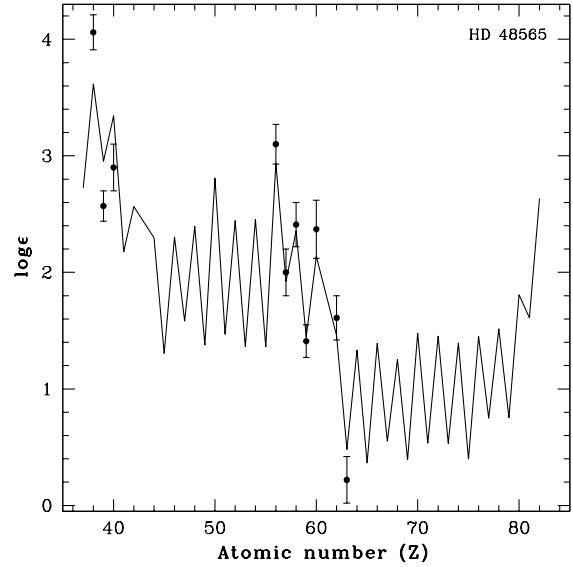


Figure 12. Solid curve represent the best fit for the parametric model function $\log \epsilon = A_s N_{si} + A_r N_{ri}$, where N_{si} and N_{ri} represent the abundances due to s- and r-process respectively (Arlandini et al. 1999, Stellar model, scaled to the metallicity of the star). The points with errorbars indicate the observed abundances in HD 48565.

position of CEMP-s stars is also explained considering a binary picture, as in the case of CH stars. Two subgiant CH stars and three objects from the CH star catalogue, i.e. HD 16458 ([Ba/Fe]=1.18, [Ba/Eu]=0.52), HD 48565 ([Ba/Fe]=1.52, [Ba/Eu]=1.23), HD 201626 ([Ba/Fe]=2.12), satisfy this criterion for CEMP-s stars; among these three the first two are also listed in the Ba star catalogue. CH stars and Ba stars are known to show enhanced abundances of carbon and heavy elements. Barium stars are generally believed to be the metal-rich population I analogues of CH stars. Allen & Barbuy (2006a,b) have concluded that bar-

ium stars also have same s-process signatures of AGB stars similar to CH stars. Peculiar abundances of heavy elements observed in barium stars are believed to be the result of a mass transfer process and can be explained with the help of a binary picture including low-mass AGB stars (Jorissen & Van Eck (2000)).

The relationship between CEMP-s and CEMP-r/s stars are not clearly understood; there are however speculations that the progenitors of the CEMP-s and CEMP-r/s class may be one and the same (TP-AGB) (Tsangarides 2005). None of the four stars for which we could measure both Ba

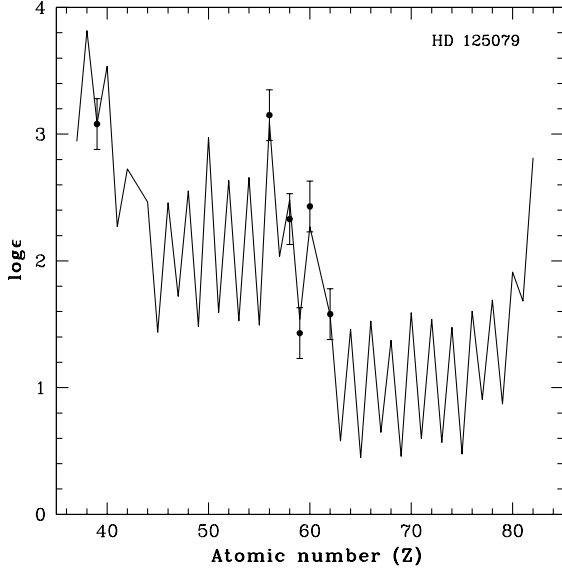


Figure 13. Solid curve represent the best fit for the parametric model function $\log \epsilon = A_s N_{si} + A_r N_{ri}$, where N_{si} and N_{ri} represent the abundances due to s- and r-process respectively (Arlandini et al. 1999, Stellar model, scaled to the metallicity of the star). The points with errorbars indicate the observed abundances in HD 125079.

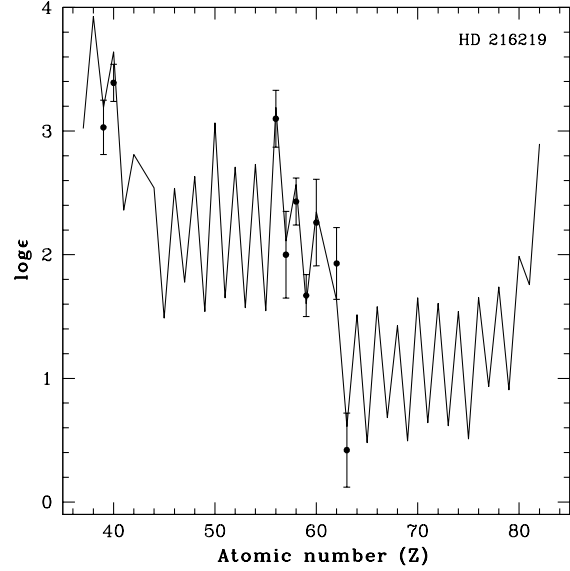


Figure 14. Solid curve represent the best fit for the parametric model function $\log \epsilon = A_s N_{si} + A_r N_{ri}$, where N_{si} and N_{ri} represent the abundances due to s- and r-process respectively (Arlandini et al. 1999, Stellar model, scaled to the metallicity of the star). The points with errorbars indicate the observed abundances in HD 216219.

and Eu abundances are found to satisfy the criterion of Beers & Christlieb (2005) for CEMP-r/s stars.

Three of our program stars HD 16458, 201626, and 216219 with $[\text{Ba}/\text{Fe}] > 1$, are known to be confirmed binaries with periods 2018 days, 1465 days and 3871 days respectively (McClure (1984, 1997), McClure & Woodsworth 1990). Long-term radial velocity monitoring of 10 years for the sub-giant CH star HD 4395 shows a radial velocity variation of -4 km s^{-1} indicating its binarity (McClure 1983, 1984, 1997). Our radial velocity estimate differs by 6 km s^{-1} from the literature value. This object however gives $[\text{Ba}/\text{Fe}] = 0.79$ and does not satisfy Beers & Christlieb (2005) criterion for CEMP-s stars.

The chemical composition of HD 81192 with $[\text{Ba}/\text{Fe}] = 0.13$, is peculiar, (i.e., it is enriched) in heavy elements of Nd and Sm and shows near-solar abundances for Ba, La, and Ce. This object shows a mild enhancement of Sr with $[\text{Sr}/\text{Fe}] = 0.58$. For CH and CEMP-s stars estimated $[\text{hs}/\text{Fe}]$ are in general ≥ 1 , where hs represents the heavy s-process elements and ls represents the light s-process elements. This condition is also not satisfied by this object. The binary status of this object is not known; the object does not seem to represent a typical CH star as far as its chemical composition is concerned.

HD 5395, with estimated $[\text{Ba}/\text{Fe}] \sim 0.13$, $[\text{Eu}/\text{Fe}] \sim 0.34$ and $[\text{Ba}/\text{Eu}] \sim -0.31$ also does not seem to belong either to the group of CH stars or CEMP-r/s stars. However, heavy elements Pr and Nd are found to be overabundant with $[\text{Pr}/\text{Fe}]$ and $[\text{Nd}/\text{Fe}]$ values of 0.79 and 0.74 respectively. Sr and La are also found to be mildly overabundant with $[\text{Sr}/\text{Fe}] \sim 0.26$ and $[\text{La}/\text{Fe}] \sim 0.24$. The abundance of HD 5395 is however consistent with one of the characteristic

properties of CH stars, i.e. the 2nd peak s-process elements are more abundant than the first-peak s-process elements.

Estimated values of $[\text{Ba}/\text{Fe}]$ for the objects HD 188650 and 214714 are respectively ~ -0.01 and -0.31 . Abundance of Eu could not be estimated for these two objects from our spectra. Except for Pr ($[\text{Pr}/\text{Fe}] = 0.57$) and Nd ($[\text{Nd}/\text{Fe}] = 0.39$) all other heavy elements i.e., Y, Ce and Sm show near-solar values for HD 188650. Similarly, HD 214714 shows a near-solar value for Ce. While Y is overabundant with $[\text{Y}/\text{Fe}] = 0.22$, Zr is found to be underabundant with $[\text{Zr}/\text{Fe}] = -0.28$ in this object. Pr, Nd and Sm are overabundant with $[\text{Pr}/\text{Fe}] = 0.93$, $[\text{Nd}/\text{Fe}] = 0.36$ and $[\text{Sm}/\text{Fe}] = 0.46$. It is possible that the objects that show mild enhancement of heavy elements such as Pr, Nd etc., their origin could be from material that are pre-enriched with such heavy elements. CH stars are known as low-mass high velocity objects, however our estimated stellar masses for HD 188650 and HD 214714 are much higher than solar values with $4.0 M_{\odot}$ and $3.5 M_{\odot}$ respectively (Table 12).

Several authors have used $[\text{hs}/\text{ls}]$ as a good indicator of s-process efficiency and used these values for classification of CH stars. For example Bisterzo et al. (2012) classified the stars with $[\text{hs}/\text{Fe}]$ value ≥ 1.5 as S II stars and those with $[\text{hs}/\text{Fe}]$ value ≤ 1.5 as S I stars. In our sample three objects belong to S II category according to these criteria.

Our parametric model based study also gives higher values for the component coefficients corresponding to contributions coming from the s-process than those from the r-process (Table 13) indicating that the s-process is the dominant one for the production of heavy element in the objects HD 48565, 125079, and 216219.

We thank the referee B. Barbuy, for her valuable suggestions which have improved the paper considerably. This work made use of the SIMBAD astronomical database, operated at CDS, Strasbourg, France, and the NASA ADS, USA. DK was a junior research fellow with the DST project NO. SR/S2/HEP-09/2007 during the early part of this work and currently a CSIR-senior research fellow. Funding from DST and CSIR are gratefully acknowledged.

REFERENCES

- Abate C., Pols O. R., Izzard R. G., Mohamed S. S., de Mink S. E., 2013, *A&A*, 552, 26
- Allen D. M., Barbuy B., 2006a, *A&A*, 454, 895
- Allen D. M., Barbuy B., 2006b, *A&A*, 454, 917
- Alonso A., Arribas S., Martinez-Roger C., 1996 *A&A*, 313, 873
- Alonso A., Arribas S., Martinez-Roger C., 1999, *A&AS*, 140, 261
- Aoki et al. 2001, *Apj*, 561, 346
- Aoki W., Ryan S. G., Norris J. E., Beers T. C., Ando H., Iwamoto N., Kajino T., Mathews G. J., Fujimoto M. Y., 2001, *ApJ*, 561, 346
- Aoki W., Norris J. E., Ryan, S. G., Beers, T. C., Ando, H., 2002, *ApJ*, 567, 1166
- Aoki W., Ryan S. G., Norris, J. E., Beers T. C., Hiroyasu, A., Tsangarides S. 2002, *ApJ*, 580, 1149
- Aoki W. et al., 2005, *ApJ*, 632, 611
- Aoki W., Beers T. C., Christlieb N., Norris J. E., Ryan S. G., Tsangarides S. 2007, *ApJ*, 655, 492
- Arlandini C., K ppeler F., Wisshak K., Gallino R., Lugaro M., Busso M., Straniero O., 1999, *ApJ*, 525, 886
- Asplund M., Grevesse N., Sauval A. J., 2005, in Barnes T. G., III, Bash F. N., eds, *ASP Conf. Ser. Vol. 336, Cosmic Abundances as Records of Stellar Evolution and Nucleosynthesis*. Astron. Soc. Pac., San Francisco, p. 25
- Baird, S.R., Roberts, W.J., Snow, T.P., Waller, W., 1975, *PASP*, 87, 385
- Barbuy B., Spite M., Spite F., Hill V., Cayrel R., Plez B., Petitjean P., 2005, *A&A*, 429, 1031
- Bartkevicius A., 1996, *BaltA*, 5, 217
- Baumüller D., Gehren T., 1997, *A&A*, 325, 1088
- Baumüller D., Butler K., Gehren T., 1998, *A&A*, 338, 637
- Beers T.C., Christlieb N., 2005, *ARA&A*, 43, 531
- Bidelman W. P., 1957, *PASP*, 69, 573
- Bidelman W. P., Astron. J, 1981, 86, 553
- Bisterzo S., Gallino R., Straniero O., Cristallo S., Kppeler F., 2012, *MNRAS*, 422, 849
- Bond H. E., 1974, *ApJ*, 194, 95
- Busso M., Gallino R., Lambert D. L., Travaglio C., Smith V. V., 2001, *ApJ*, 557, 802
- Cayrel R. et al., 2004, *A&A*, 416, 1117
- Christlieb N., Green P. J., Wisotzki L., Reimers D., 2001b, *A&A*, 375, 366
- Cottrell P.L., Sneden, C., 1986, *A&A* 161, 314
- De Medeiros J.R., Mayor, M. 1999, *A&AS*, 139, 433
- Fernandez-Villacanas J.L., Rego M., Cornide M., 1990, *AJ* 99, 1961
- Girardi L., Bressan A., Bertelli G., Chiosi C., 2000, *A&AS* 141, 371.
- Goswami A., 2005, *MNRAS*, 359, 531
- Goswami A., Wako A., Beers T. C., Christlieb N., Norris J., Ryan S. G., Tsangarides S. 2006, *MNRAS*, 372, 343
- Goswami A., Bama P., Shantikumar N. S., Devassy D., 2007, *BASI*, 35, 339
- Goswami A., Karinkuzhi D. & Shantikumar N. S., 2010b, *MNRAS*, 402, 1111
- Goswami A., Wako A., 2010, *MNRAS*, 404, 253
- Goswami A., Karinkuzhi D., 2013, *A&A*, 549, 68
- Goswami A., Subramania Athiray P., Kurinkuzhi D., in *Recent Advances in Spectroscopy: Astrophysical, Theoretical and Experimental Perspectives* eds. Chaudhuri, R. K. et al., *Astrophysics and Space Science Proceedings*, p 211, Springer Verlag, 2010a
- Jonsell K., Barklem P. S., Gustafsson B., Christlieb N., Hill V., Beers T. C., Holmberg J., 2006, *A&A*, 451, 651
- Jorissen A., van Eck S., 2000, *IAUS*, 177, 259
- Krishnaswamy K., Sneden C., 1985, *PASP* 97, 407.
- Kurucz R. L., 1995a, in *ASP Conf. Proc. 78, Astrophysical Applications of Powerful New Databases*, ed. S. J. Adelman & W. L. Wiese (San Francisco:ASP), 205
- Kurucz R. L., 1995b, in *ASP Conf. Proc. 81, Laboratory and Astronomical High Resolution Spectra*, ed. A. J. Sauval, R. Blomme, N. Grevesse (San Francisco:ASP), 583
- Lawler J. E., Bonvallet G., Sneden C., 2001, *Apj*, 556, 452
- Lü, P. K. 1991, *AJ*, 101, 2229
- Lucatello S., Gratton R. G., Beers T. C., Carretta E., 2005, *ApJ*, 625, L833
- Luck R.E., 1991, *ApJS* 75, 579.
- Luck R.E., Bond H.E., 1982, *ApJ*, 259, 792
- Luck R.E., Bond H.E., 1983, *ApJ*, 271, L75
- Luck R.E., Bond H.E., 1985, *ApJ*, 292, 559
- Luck R.E., Bond H.E., 1991, *ApJS*, 77, 515
- McClure R. D., 1983, *ApJ*, 268, 264
- McClure R. D., 1984, *ApJ*, 280, L31
- McClure R. D., Woodsworth W., 1990, *ApJ*, 352, 709
- McClure R. D., 1997, *PASP*, 109, 536
- McWilliam A., 1990, *ApJS* 74, 1075.
- McWilliam A., Preston G. W., Sneden C., Searle L., 1995, *AJ*, 109, 2757
- McWilliam A., 1998, *Aj*, 115, 1640
- Massaroti A., Latham, D.W., Stefanik, R.P., Fogel, J. 2008, *AJ*, 135, 209
- Morgan W. W., Keenan P. C., Kellman E., 1943, *QB881*, M6
- Moultaka J., Ilovaisky S. A., Prugniel P., Soubiran C., 2004, *PASP*, 116, 693
- Mucciarelli A., Caffau E., Freytag B., Ludwig H., Bonifacio P., 2008, *A&A*, 484, 841
- Nordstroem B. et al. 2004, *A&A*, 418, 989
- Norris J. E., Ryan S.G., Beers, T. C. 1997a, *ApJ*, 488, 350
- Norris J. E., Ryan S.G., Beers T. C. 1997b, *ApJ*, 489, L169
- Norris J. E., Ryan S.G., Beers T. C., Aoki, W & Ando H., 2002, *ApJ*, 569, L107
- North P., Berthet S., Lanz T., 1994, *A&A* 281, 775
- Prochaska J. X., McWilliam A., *ApJ*, 537, L57
- Ramirez I., Melendez J., 2004, *ApJ*, 609, 417
- Shetrone M.D., Sneden C. and Pilachowski C.A., 1993, *PASP*, 105, 337
- Smith V.V., 1984, *A&A* 132, 326
- Smith V.V., Lambert D.L., 1986, *ApJ* 303, 226.
- Smith V.V., Coleman H., Lambert D.L., 1993, *ApJ* 417, 287
- Sneden C., 1973, PhD thesis, Univ of Texas at Austin
- Sneden C., Bond H. E., 1976, *ApJ*, 204, 810
- Sneden C., McWilliam A., Preston G. W., Cowan J.J., Burris D. L., Armosky B. J., 1996, *Apj*, 467, 819
- Tsangarides S. A., 2005, PhD thesis, Open University
- Tomkin, J., Lambert, D.L., 1983, *ApJ* 273, 722
- Vanture A. D., 1992a, *AJ*, 103, 2035
- Vanture A. D., 1992b, *AJ*, 104, 1986
- Vanture A. D., 1992c, *AJ*, 104, 1997
- Wallerstein, G., Greenstein, J.L., 1964, *ApJ* 139, 1163
- Wilson R. E. 1953, *GCRV*, C, 0
- Worley C. C, Hill V., J. Sobeck J., Carretta E., *A&A*, 2013, 553, A47